An Intermediary Role of proHB-EGF Shedding in Growth Factor-induced c-Myc Gene Expression

DAISUKE NANBA,[1] HIROFUMI INOUE,[1] YUKA SHIGEMI,[1] YUJI SHIRAKATA,[2] KOJI HASHIMOTO,[2] AND SHIGEKI HIGASHIYAMA[1,3*]

[1]Department of Biochemistry and Molecular Genetics, Ehime University Graduate School of Medicine, Shitsukawa, Toon, Ehime, Japan

[2]Department of Dermatology, Ehime University Graduate School of Medicine, Shitsukawa, Toon, Ehime, Japan

[3]PRESTO, JST, Japan

Activation of growth factor receptors by ligand binding leads to an increased expression of c-Myc, a transcriptional regulator for cell proliferation. The activation of transcriptional factors via the activated receptors is thought to be the main role of c-Myc gene expression. We demonstrate here that epidermal growth factor receptor (EGFR)- and fibroblast growth factor receptor (FGFR)-mediated c-Myc induction and cell cycle progression in primary cultured mouse embryonic fibroblasts (MEFs) are abrogated by knockout of the heparin-binding EGF-like growth factor (Hb-egf) gene, or by a metalloproteinase inhibitor, although molecules downstream of the receptors are activated. Induction of c-Myc expression by EGF or basic FGF is recovered in Hb-egf-depleted MEFs by overexpression of wild-type proHB-EGF, but no recovery was observed with an uncleavable mutant of proHB-EGF. The uncleavable mutant also inhibited EGF-induced acetylation of histone H3 at the mouse c-Myc first intron region, which could negatively affect transcriptional activation. We conclude that signal transduction initiated by generation of the carboxyl-terminal fragment of proHB-EGF (HB-EGF-CTF) in the shedding event plays an important intermediary role between growth factor receptor activation and c-Myc gene induction.

J. Cell. Physiol. 214: 465–473, 2008. © 2007 Wiley-Liss, Inc.

Growth factors stimulate quiescent cells into DNA synthesis. The transcription factor encoded by the c-Myc gene is expressed in a strictly growth factor-dependent manner in quiescent cells (Obaya et al., 1999) and directs gene transcription associated with the transition from quiescence to proliferation. For example, c-Myc induces a number of target molecules involved in G1 phase entry into the cell cycle, including Cdc25A, cyclin D2, CDK4, Cul1, and E2F2 (Galaktionov et al., 1996; Leone et al., 1997; Bouchard et al., 1999; Hermeking et al., 2000), supporting the conclusion that c-Myc plays a central role in cell cycle progression as an upstream regulator of cell cycle regulatory molecules. Indeed, c-Myc null cells are able to survive, but display a marked lengthening of both the G1 and G2 phases of the cell cycle. Although the duration of S phase in c-Myc null cells remains unchanged, the G0 to S phase transition is also significantly delayed (Mateyak et al., 1997).

A key step for signaling through the epidermal growth factor receptor (EGFR) is the release of mature ligands such as heparin-binding EGF-like growth factor (HB-EGF) from their membrane-anchored precursor forms, a process referred to as "ectodomain shedding" (Blobel, 2005; Higashiyama and Nanba, 2005). The HB-EGF precursor (proHB-EGF) is cleaved by members of the "a disintegrin and metalloprotease" (ADAM) protease family (Asakura et al., 2002; Blobel, 2005; Higashiyama and Nanba, 2005), yielding the carboxyl terminal fragment of proHB-EGF (HB-EGF-CTF) in parallel with the production of HB-EGF. We have previously characterized HB-EGF-CTF as a novel intracellular signaling molecule that is acquired post-translationally and translocated into the nucleus, where it binds to and inactivates the promyelocytic leukemia zinc finger protein (PLZF) (Nanba et al., 2003). PLZF is a transcriptional repressor that suppresses transcription of genes such as c-Myc, cyclin A2, and HoxD11 (Yeyati et al., 1999; Barna et al., 2000; McConnell et al., 2003). Thus, shedding of proHB-EGF

participates in activation of two independent signal transduction pathways: signaling from EGFR after engagement of the shed growth factor, and a HB-EGF-CTF-mediated signaling (Higashiyama and Nanba, 2005). Here, we demonstrate that HB-EGF-CTF signaling is involved in growth factor-induced c-Myc expression.

Materials and Methods
Materials

12-o-tetradecanoylphorbol-13-acetate (TPA) was purchased from WAKO Pure Chem. Ind., Ltd. (Osaka, Japan). KB-R7785 (Asakura

WILEY
InterScience®
DISCOVER SOMETHING GREAT

et al., 2002) and EGFR-neutralizing antibodies were obtained from Carna Biosciences, Inc. (Kobe, Japan) and Immuno-Biological Laboratories Co., Ltd. (Takasaki, Japan), respectively. Recombinant EGF and basic fibroblast growth factor (bFGF) were purchased from R&D Systems, Inc. (Minneapolis, MN).

Cell culture

The fibrosarcoma cell line HT1080 was cultured in Eagle minimum essential medium (EMEM) (Nikken Bio Medical Laboratory, Kyoto, Japan) with 10% fetal calf serum (FCS), 100 units of penicillin G potassium, and 100 µg of streptomycin sulfate per milliliter. The culture of primary human epidermal keratinocytes was prepared as described previously (Hashimoto et al., 1994). E13.5 embryos from loxHB-EGF mice were used to generate mouse embryonic fibroblasts (MEFs). MEFs were maintained in Dulbecco's modified Eagle medium (DMEM) (Nikken) supplemented with 10% FCS, 100 units of penicillin G potassium, and 100 µg of streptomycin sulfate per milliliter. Quiescent MEFs were prepared by serum starvation for 3 days. All cells were cultured in a humidified 37 C/ 5% CO_2 incubator.

Ribonuclease protection assay (RPA)

Total RNA was isolated from keratinocytes (1.0×10^6 cells) or MEFs (2.0×10^6 cells) with Trizol reagent (Invitrogen, Carlsbad, CA). Riboprobes were labeled with digoxigenin (DIG) using the DIG RNA labeling kit (Roche Diagnostics, Basel, Switzerland) according to the manufacturer's protocol. Thirty micrograms of total RNA harvested from cells cultured under each condition were hybridized with DIG-labeled probes. RNase treatment and gel resolution of protected probes were performed according to the manufacturer's protocol with the RPAIII kit (Ambion, Austin, TX). Each value (c-Myc/Gapdh) was normalized using the value for non-treated cells as taken to be one in each experiment. The values (means ± SD) were determined based on results in at least three independent experiments. P-values were obtained from Student's t-test.

Immunoprecipitation and immunoblotting

Immunoprecipitation and immunoblotting of cell lysates was performed as described previously (Goishi et al., 1995; Nanba et al., 2003). The primary antibodies used were as follows: mouse monoclonal antibodies to phospho-EGFR (Upstate, Billerica, MA); rabbit polyclonal antibodies to EGFR (Santa Cruz Biotechnology, Santa Cruz, CA), Erk1/2, phospho-Erk1/2 (Cell Signaling

Technology, Lexington, KY), anti-β-actin (SIGMA, St. Louis, MO) and anti-HB-EGF-CTF antibodies (H1). Incubations of 1 h were performed with two secondary antibodies: HRP-conjugated goat anti-mouse and rabbit IgG (Promega, Madison, WI).

ProHB-EGF-AP shedding assay

HT1080 cells stably expressing alkaline phosphatase (AP)-tagged proHB-EGF (Asakura et al., 2002) were seeded in 24-well plates at a density of 1.0×10^5 cells per well and incubated for 24 h. Recombinant EGF (final 1–50 ng/ml), and bFGF (final 1–50 ng/ml) were added and the plates were incubated for a further 1 h. pAP-HB-EGF plasmids were transiently transfected into MEFs using a MEF Nucleofector kit (Amaxa Biosystems, Gaithersburg, MD). Twenty-four hours after transfection, the cells were treated with KB-R7785 (final 10–20 µM) and TPA (final 100 nM). Aliquots (100 µl each) of the conditioned media were used to measure AP activity as described previously (Tokumaru et al., 2000).

Immunofluorescence microscopy and visualization of the fluorescent signal intensity

Immunofluorescence microscopy of human keratinocytes using a rabbit polyclonal antibody to HB-EGF-CTF (Miyagawa et al., 1995) was performed as described previously (Nanba et al., 2003). We visualized the intensity of the fluorescent signal in each picture using Scion image (Scion Corporation, Frederick, MD).

Adenovirus construction and infection

Adenovirus vectors carrying genes encoding LacZ, green fluorescent protein (GFP), AP-tagged or non-tagged proHB-EGF, and uncleavable proHB-EGF were prepared using an adenovirus expression kit (Takara Biomedicals, Otsu Japan). An adenovirus expressing Cre recombinase (Kanegae et al., 1995) under the control of the CAG promoter (Niwa et al., 1991) was obtained from RIKEN BRC (Tsukuba, Japan). Purified, concentrated, and titer-checked viruses were applied to cells at a multiplicity of infection (MOI) of 100.

PCR, RT-PCR, and quantitative PCR analysis

Deletion of the mouse Hb-egf gene, mRNA expression of EGFR ligands, and Plzf in MEFs were confirmed by PCR and RT-PCR analysis, respectively. Primers are shown in Table 1. Quantitative PCR was performed using the ABI Prism 7700 sequencer detection system (Applied Biosystems, Foster, CA) with TaqMan Gene Expression Assay kits (Applied Biosystems) for mouse c-Myc

TABLE 1. Primer sequences for PCR and RT-PCR analysis

Primer	Sequence
loxHB-EGF (forward)	5'-CGGACAGTGCCTTAGTGGAACCTC-3'
loxHB-EGF (reverse)	5'-GCTTCTTCTTAGGAGGGAATCTTGGC-3'
Mouse Hb-egf (forward)	5'-TGCCGTCGGTGATGCTGAACT-3'
Mouse Hb-egf (reverse)	5'-GGTTCAGATCTGTCCCTTCCAAGTC-3'
Mouse Tgf-α (forward)	5'-GGAATTCCTAGCGCTGGGTATCCTGTTA-3'
Mouse Tgf-α (reverse)	5'-CAAGCTTACCACCACCAGGGCAGTGATG-3'
Mouse Amphiregulin (forward)	5'-GCAATTGTCATCAAGATTACTTTGG-3'
Mouse Amphiregulin (reverse)	5'-TCTGTTTCTCCTTCATATTCCCTG-3'
Mouse Epiregulin (forward)	5'-GGAATTCTGACGCTGCTTTGTCTAGGTT-3'
Mouse Epiregulin (reverse)	5'-CAAGCTTTATGCATCCAGCGGTTATGAT-3'
Mouse Plzf (forward)	5'-TCAAGAGCCACAAGCGCATCCACA-3'
Mouse Plzf (reverse)	5'-CGAGGCACCGTTGTGTGTTCTCA-3'
Mouse GAPDH (forward)	5'-CGTATTGGGCGCCTGGTCACCAG-3'
Mouse GAPDH (reverse)	5'-TCGCTCCTGGAAGATGGTGATGGG-3'
Region I (forward)	5'-GTGCAATGAGCTCGATGAAGGAAG-3'
Region I (reverse)	5'-GTCTTCTTATTCCGGACTCCTCG-3'
Region II (forward)	5'-TTACTGGACTGCGCAGGGAG-3'
Region II (reverse)	5'-CCACGTATACTTGGAGAGCCACTT-3'
Region III (forward)	5'-GGTAAGCACAGATCTGGTGGTCTT-3'
Region III (reverse)	5'-AAGTCAGAAGCTACGGAGCCTTCT-3'
Region IV (forward)	5'-GACGGCGCGAATAGGGAC-3'
Region IV (reverse)	5'-CTACTATCAGTGACGCTCGTCG-3'
zf5-binding region (forward)	5'-TATTGTGTGGAGCGAGGCAGCT-3'
zf5-binding region (reverse)	5'-GTGTAAACAGTAATAGCGCAGCATGAATTAAC-3"

mRNA. The values (means ± SD) were determined based on results in at least three independent experiments. P-values were obtained from Student's t-test.

Cell cycle analysis

Cell cycle analysis was performed as described previously (Nanba et al., 2003), using a FACScan instrument (Becton & Dickinson, Franklin Lakes, NJ).

Chromatin immunoprecipitation (ChIP) assay

Mock-treated or EGF-stimulated cells were formaldehyde crosslinked, harvested, and disrupted by Bioruptor (COSMOBIO, Tokyo, Japan), following the method in the EZ ChIP manual (Upstate). Immunoprecipitation was performed with anti-acetylated histone H3 (Upstate), anti-PLZF (Calbiochem, San Diego, CA), or anti-FLAG antibodies (SIGMA). The primers used in this assay are shown in Table 1.

Results
Effect of cell growth factors on proHB-EGF shedding

Shedding of proHB-EGF occurs following stimulation by injury, UV, oxidants, phorbol esters, GPCR agonists, etc. (Takenobu et al., 2003; Higashiyama and Nanba, 2005). To investigate whether stimulation of growth factors such as EGF and bFGF induces shedding of proHB-EGF, we performed an AP-tagged assay with HT1080 cells that were stably transfected with AP-tagged proHB-EGF (Tokumaru et al., 2000). Increasing AP activity in the medium, indicating release of HB-EGF, was detected after stimulation of both EGF and bFGF (Fig. 1A). We also confirmed the production of HB-EGF-CTF after stimulation with these growth factors (Fig. 1B).
A metalloprotease inhibitor, KB-R7785, effectively blocked growth factor-induced proHB-EGF shedding, indicating involvement of metalloproteases in the shedding mechanism, as reported previously (Tokumaru et al., 2000; Nanba et al., 2003; Shirakata et al., 2005) (Fig. 1A). Moreover, we examined the localization of endogenous HB-EGF-CTF in human keratinocytes. Accumulation of endogenous HB-EGF-CTF in nuclei (Nanba et al., 2003) was markedly enhanced by the addition of bFGF, and this was inhibited by KB-R7785 (Fig. 2).

Effects of an inhibitor of proHB-EGF shedding on c-Myc expression induced by EGF

We have previously shown that HB-EGF-CTF, which is produced after shedding, regulates the expression of cyclin A2 by inhibition of the PLZF repressor protein (Nanba et al., 2003). PLZF has also been known to inhibit the expression of human c-Myc (McConnell et al., 2003). Therefore, we suspected that shedding of proHB-EGF and subsequent production of HB-EGF-CTF may control human c-Myc gene expression by abrogation of PLZF function. To examine the involvement of proHB-EGF shedding in EGF-induced c-Myc expression, we first performed an RPA with human primary cultured keratinocytes with intrinsic expression of HB-EGF, EGFR, and PLZF. Treatment with KB-R7785, a potent proHB-EGF shedding inhibitor (Asakura et al., 2002), resulted in a decreased expression of c-Myc mRNA under growth medium conditions (MDCB153 medium supplemented with insulin and bovine hypothalamic extract) to close to the basal level (Fig. 3A), whereas KB-R7785 did not affect phosphorylation of EGFR and Erk1/2, even when recombinant EGF was present (Fig. 3B). Treatment with a combination of KB-R7785 and anti-EGF receptor antibodies appeared to lead to even greater suppression of the c-Myc gene. These results imply that the activation of EGFR signaling brought about full induction of c-Myc expression with shedding of proHB-EGF.
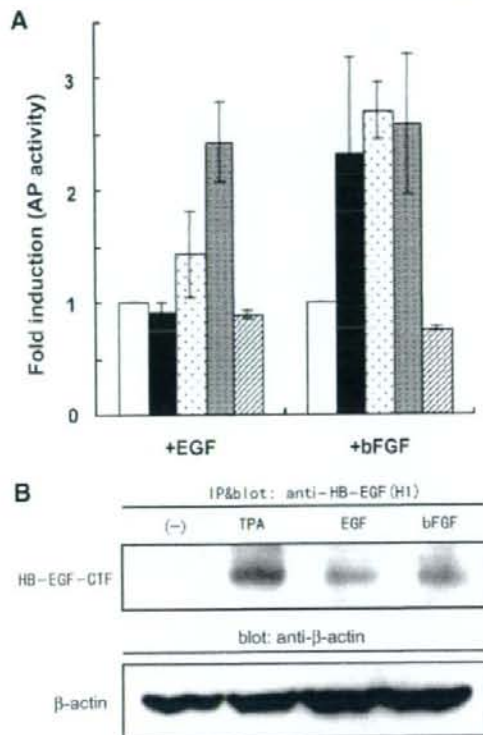

Fig. 1. Induction of proHB-EGF shedding by stimulation of EGF and bFGF. AP-tagged proHB-EGF was stably expressed in HT1080 fibrosarcoma cells. A: These cells were treated with various concentrations of EGF or bFGF for 1 h, and the AP activity was analyzed in each medium. Open bars, no stimulation; closed bars, 1 ng/ml; dotted bars, 10 ng/ml; shaded bars, 50 ng/ml; slashed bars, 50 ng/ml of growth factor and 10 µM of KB-R7785. All experiments were performed independently in triplicate. B: The lysates were collected from the above cells after each stimulation, and immunoprecipitated with anti-HB-EGF-CTF antibodies. After that, SDS–PAGE and immunoblotting with the above antibodies (upper part) were performed. β-actin in each cell lysate was detected with anti-β-actin antibodies as an indicator of protein loading (lower part).

To evaluate whether this event is species specific, we also examined expression of c-Myc in MEFs. mRNA of c-Myc was induced by stimulation of EGF and treatment with KB-R7785 partially suppressed c-Myc expression (Fig. 3C), but had no remarkable effect on phosphorylation of EGFR and Erk1/2 under treatment of KB-R7785 in MEFs (Fig. 3D). TPA is one of the strongest inducers of proHB-EGF shedding. To confirm the blocking effect of shedding by the metalloproteases inhibitor, KB-R7785, in MEFs, we performed proHB-EGF-AP shedding assay with adenovirus infection system (Fig. 3E). KB-R7785 even blocked the induction of proHB-EGF shedding by TPA.

Reduction of EGF-induced c-Myc gene expression in proHB-EGF-depleted mouse embryonic fibroblasts

To define the transcriptional regulation of c-Myc by HB-EGF more precisely, we generated Hb-egf-deficient MEFs using Cre/loxP technology (Fig. 4A). MEFs were isolated from loxHB-EGF
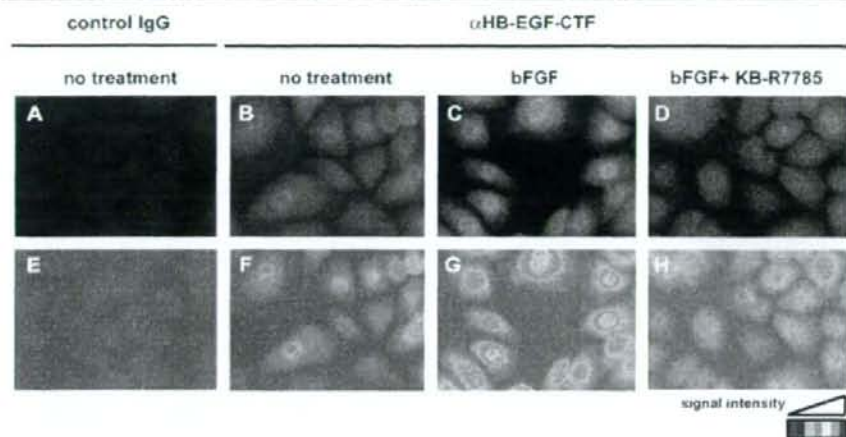
Fig. 2. Intracellular localization of endogenous HB-EGF-CTF in human keratinocytes, determined by fluorescent microscopy. Human keratinocytes were stimulated with 10 ng/ml bFGF for 30 min, after which they were fixed and stained with normal rabbit IgG or anti-HB-EGF-CTF antibodies. A, B, E, and F are images taken before stimulation; (C) and (G) are images collected after stimulation; and (D) and (H) show the effect of KB-R7785 treatment before stimulation with bFGF. A and E, normal rabbit IgG; B–D and F–H, anti-HB-EGF-CTF antibodies. Parts E–H show analytical data for A–D, respectively, determined using Scion Image.
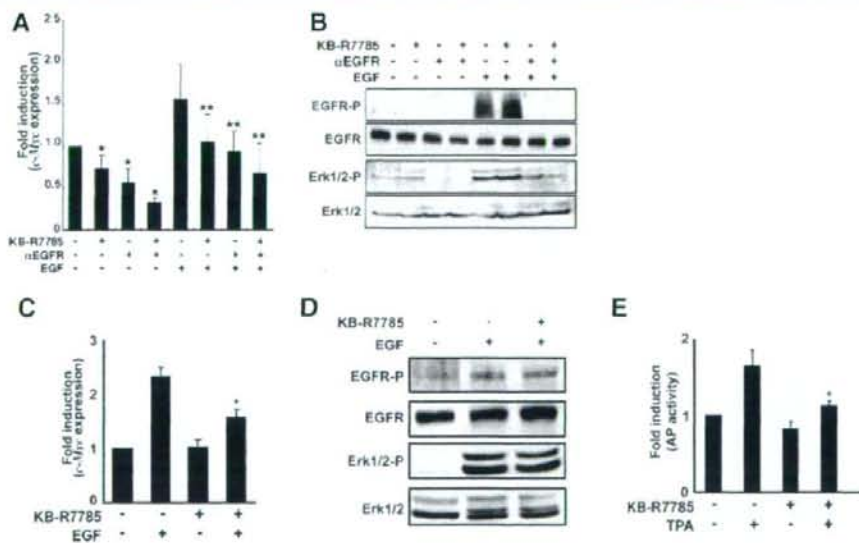

Fig. 3. Involvement of shedding of proHB-EGF in c-Myc transcription by human primary cultured keratinocytes and mouse embryonic fibroblasts. A: Analysis of c-Myc mRNA expression in keratinocytes by RPA. The intensities of the bands for c-Myc and Gapdh mRNA were measured by densitometry. In some cases, the keratinocytes were pretreated with 10 μM of KB-R7785 and/or 10 μg/ml of EGFR-neutralizing antibody for 1 h. Some of the cultures were further treated with 10 ng/ml of EGF for 1 h. Expression of Gapdh mRNA was examined as a control. *P < 0.05 versus non-treated keratinocytes (lane 1) and **P < 0.05 versus EGF-treated keratinocytes (lane 5). B: Phosphorylation of EGFR (middle parts) and Erk-1/-2 (lower parts) in keratinocytes was observed in a Western blot assay. C: Analysis of c-Myc mRNA expression in MEFs by RPA. The intensities of the bands for c-Myc and Gapdh mRNA were measured by densitometry. D: Detection of EGF signaling through the EGF receptor by an IP-Western assay. All experiments were performed independently in triplicate. E: Effect of KB-R7785 on shedding of proHB-EGF in MEFs. MEFs transiently expressed with AP-proHB-EGF were stimulated with 100 nM of 12-o-tetradecanoylphorbol-13-acetate (TPA). Before stimulation with TPA, the cells were treated with 20 μM of KB-R7785. *P < 0.05 versus EGF-treated MEFs. A and C, The expression level of c-Myc was normalized using the level of Gapdh, and the fold induction is shown on the basis of the expression ratio relative to no treatment.

mice (Iwamoto et al., 2003; Shirakata et al., 2005) and infected with adenoviruses encoding either Cre or GFP. Deletion of the Hb-egf gene and the absence of its mRNA transcript were confirmed in Cre recombinase-expressing MEFs (HB$^{-/-}$ cells); in contrast, the gene and transcript were retained in GFP-expressing MEFs (HB$^{+/+}$ cells) (Fig. 4A–C). HB-EGF protein production in HB$^{+/+}$ and HB$^{-/-}$ cells was detected by Western blotting (Fig. 4B, lower part). Stimulation of EGF induced c-Myc expression in quiescent HB$^{+/+}$ cells, and up-regulation of c-Myc by EGF was also attenuated in HB$^{-/-}$ cells (Fig. 4D). Strikingly, phosphorylation of EGFR and Erk1/2 was stimulated equally in response to EGF in HB$^{+/+}$ and HB$^{-/-}$ cells (Fig. 4E).

Negative effects of uncleavable mutant of proHB-EGF on c-Myc gene expression and cell cycle progression

We next performed a recovery assay with adenovirus infection of MEFs to introduce exogenous expression of wild-type proHB-EGF. Protein production by wild-type or mutant proHB-EGF in HB$^{-/-}$ cells is shown in Fig. 5A. Infection with viruses carrying the wild-type protein restored c-Myc induction in HB$^{-/-}$ cells by EGF (Fig. 5B). Although the quiescent MEFs proceeded into S phase following EGF stimulation, entry into this phase was somewhat delayed in HB$^{-/-}$ cells compared

to HB$^{+/+}$ cells with statistical significance (Fig. 5C). On the other hand, expression of an uncleavable mutant of proHB-EGF (Nanba et al., 2003) by adenovirus infection severely depressed c-Myc expression in both HB$^{-/-}$ and HB$^{+/+}$ cells (Fig. 5B). Moreover, adenovirus-driven overexpression of the uncleavable mutant completely inhibited cell cycle progression into S phase, although overproduction of wild-type proHB-EGF in HB$^{-/-}$ cells accelerated entry into S phase (Fig. 5C). It is presumably due to a potent dominant negative effect of the uncleavable form.

Elevated transcription of c-Myc was induced in quiescent MEFs stimulated with bFGF (Fig. 6A). The increased transcription of c-Myc mRNA in response to bFGF was significantly depressed in HB$^{-/-}$ cells (Fig. 6A). Expression of wild-type proHB-EGF recovered the induction of the c-Myc gene by bFGF in HB$^{-/-}$ cells, but expression of the uncleavable mutant of proHB-EGF did not do so (Fig. 6B). These data raise the possibility that the release of overexpressed HB-EGF restored c-Myc induction by bFGF. However, induction by bFGF was not inhibited by treatment with HB-EGF-neutralizing antibodies under the expression of proHB-EGF (Fig. 6B). bFGF induced quiescent MEFs into S phase, but S phase entry was delayed in HB$^{-/-}$ cells compared to HB$^{+/+}$ cells (Fig. 6C). Furthermore, expression of the uncleavable mutant markedly suppressed S phase entry, similarly to the result with EGF.
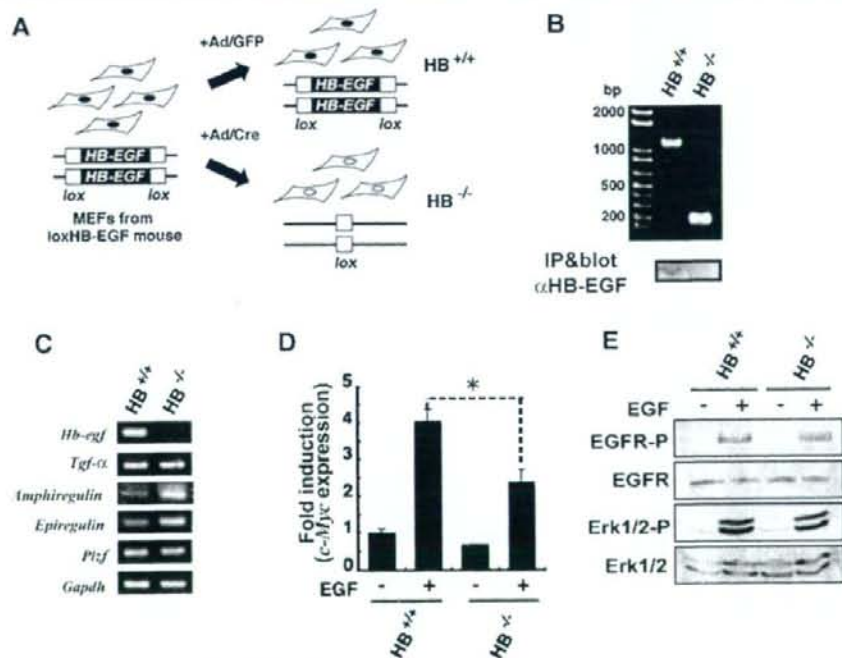

Fig. 4. Involvement of HB-EGF in c-Myc transcription induced by EGFR signaling. A: Schematic representation of generation of proHB-EGF-deficient MEFs from loxHB-EGF mice. B: The upper part shows PCR detection of the Hb-egf gene in loxHB-EGF MEFs after infection with adenoviruses expressing GFP (HB$^{+/+}$) or Cre (HB$^{-/-}$). The upper band represents the intact Hb-egf gene flanked by loxP sites, and the lower band reflects the fragment size decrease after Hb-egf gene deletion. The bottom part shows the protein level of proHB-EGF in each type of cell. Data were collected for 10^6 cells for each condition. C: RT-PCR analysis of mRNAs for EGFR ligands (Hb-egf, Tgf-α, Amphiregulin, and Epiregulin) and Plzf mRNA expression. D: Analysis of c-Myc mRNA expression in HB$^{+/+}$ and HB$^{-/-}$ cells by quantitative PCR analysis. Serum-starved MEFs were stimulated with 10 ng/ml EGF for 1 h. Expression of Gapdh mRNA was examined as a normalization control, and densitometric analysis was performed. *P < 0.05 versus HB$^{+/+}$ cells treated with EGF. E: Phosphorylation of EGFR and Erk1/2 induced by addition of EGF for 15 min in HB$^{+/+}$ and HB$^{-/-}$ cells. All experiments were performed independently in triplicate.
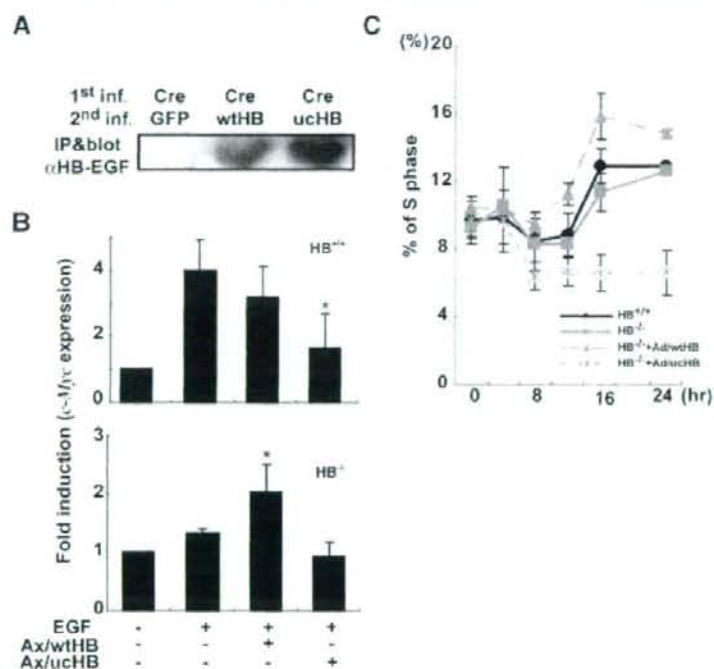
Fig. 5.   EGFR signaling-induced c-Myc transcription and cell cycle progression by expression of proHB-EGF and an uncleavable mutant. A: The protein level of each proHB-EGF in adenovirus-infected cells. Immunoprecipitation and the Western blotting assay were each performed using 10^6 cells. 1st inf. and 2nd inf. indicate first and second infection respectively. B: RPA of c-Myc transcription induced by EGF in $HB^{+/+}$ and $HB^{-/-}$ cells infected with adenoviruses encoding either proHB-EGF (Ax/wtHB) or its uncleavable mutant (Ax/ucHB). The expression level of c-Myc was normalized using the corresponding expression level of Gapdh, and fold induction is shown based on a control value of 1. C: Flow cytometry analysis of cell cycle progression in cells stimulated with EGF. All experiments were performed independently in triplicate.
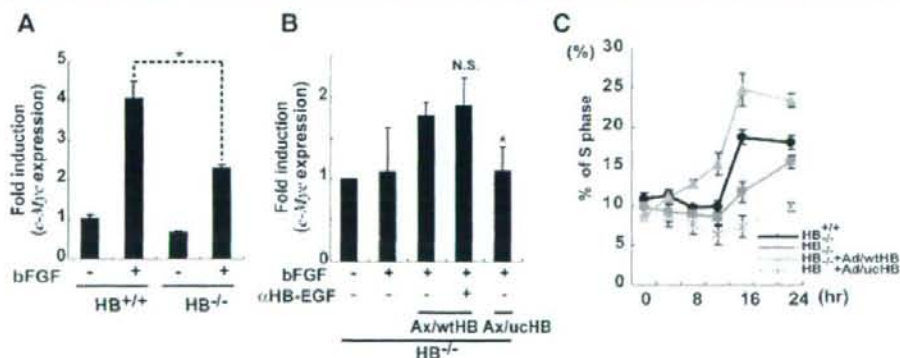

Fig. 6.   Involvement of proHB-EGF shedding in c-Myc transcription induced by bFGF. A: Quantitative PCR analysis of c-Myc transcription induced by bFGF in $HB^{+/+}$ and $HB^{-/-}$ cells. Serum-starved MEFs were stimulated with 1 ng/ml bFGF for 1 h. Expression of Gapdh mRNA was examined as a control. B: RPA of c-Myc transcription induced by bFGF in $HB^{-/-}$ cells infected with Ax/wtHB and Ax/ucHB. A HB-EGF-neutralizing antibody (αHB-EGF) was used to inhibit the function of mature HB-EGF. The expression level of c-Myc was normalized using the corresponding expression level of Gapdh, and fold induction is shown based on a control value of 1. C: Flow cytometry analysis of cell cycle progression in cells stimulated with bFGF. $^*P < 0.05$ versus $HB^{+/+}$ cells. All experiments were performed independently in triplicate.

These results suggest that proHB-EGF shedding and subsequent HB-EGF-CTF signaling can modulate bFGF signaling-induced c-Myc expression and cell cycle progression.

Epigenetic effect of uncleavable proHB-EGF on Mouse c-Myc gene promoter

We have previously reported that HB-EGF-CTF inactivates PLZF, a transcriptional repressor, by induction of translocation to the cytoplasm. On the other hand, a recent study has shown that PLZF represses expression of human c-Myc (McConnell et al., 2003). When we checked the PLZF-binding motifs in the 5 kb region from the transcriptional start site of the mouse c-Myc gene, six putative sites were found (Fig. 7A). To examine chromatin modification in MEFs infected by adenoviruses carrying GFP or the uncleavable mutant of proHB-EGF, a chromatin immunoprecipitation (ChIP) assay was performed. After stimulation with EGF, the level of acetylated histone H3 increased at the region III (Fig. 7B), where the acetylation, however, was not induced with expression of the uncleavable form of proHB-EGF. These data suggest that production of HB-EGF-CTF followed by shedding is required for histone modification. We also examined the participation of PLZF in this region in the ChIP assay. However, the fragment of the region III was not detected with anti-PLZF antibodies (data not shown). We also tried detection of this region with anti-FLAG antibodies in FLAG-tagged PLZF-overexpressed cells, but the region III was not detected again (Fig. 7C).

Discussion

Induction of c-Myc transcription by receptor tyrosine kinases (RTKs) is regulated by at least two distinct intracellular signaling pathways: the Ras/Raf/MEK/ERK (MAPK) pathway (Kerkhoff et al., 1998) and the Src pathway (Barone and Courtneidge, 1995; Chiariello et al., 2001). The MAPK pathway induces proHB-EGF shedding by the activation of metalloproteases

(Gechtman et al., 1999; Umata et al., 2001). The activated metalloproteases cleave proHB-EGF at the plasma membrane, generating both the EGFR ligand HB-EGF and the transcription-modulating protein HB-EGF-CTF (Nanba et al., 2003). The present study demonstrates that signal transduction mediated by HB-EGF-CTF modulates induction of c-Myc transcription and cell cycle progression by EGF and bFGF.

Reiss et al. provided evidence that proteolysis of transmembrane proteins on the cell surface is involved in c-Myc expression, by showing decreased expression of c-Myc in ADAM10-deficient MEFs (Reiss et al., 2005). ADAM10 cleaves N-cadherin, an event that causes redistribution of β-catenin from the plasma membrane to the cytoplasmic pool, thereby accelerating β-catenin/Tcf signaling and the resulting c-Myc expression (He et al., 1998). ADAM10 is also a sheddase for proHB-EGF and other EGFR ligand precursors (Sahin et al., 2004). Therefore, it is possible that KB-R7785, a metalloproteinase inhibitor, could inhibit the increase in c-Myc expression by blocking redistribution of β-catenin (Fig. 3A, C). However, expression of the c-Myc gene by growth factors diminished in MEFs in which the Hb-egf gene was removed by Cre recombinase (Figs. 4D, 5B, and 6A). Moreover, expression of an uncleavable mutant of proHB-EGF did not recover expression of c-Myc, rather inhibited it (Figs. 5B and 6B), suggesting that full induction of the c-Myc gene by growth factors requires shedding of proHB-EGF. CTF signaling derived from proHB-EGF may also contribute to c-Myc transcription induced by growth factors.

c-Myc participates in a variety of biological processes, including cell proliferation, differentiation, apoptosis, metabolism, and tumorigenesis (Dang, 1999; Murphy et al., 2005). We performed cell cycle analysis to determine the effects caused by a change in c-Myc expression. Delayed S phase entry was observed in Hb-egf-depleted MEFs following stimulation with either EGF or bFGF (Figs. 5C and 6C). Expression of the uncleavable mutant of proHB-EGF in the presence of the wild-type protein completely stopped the cell
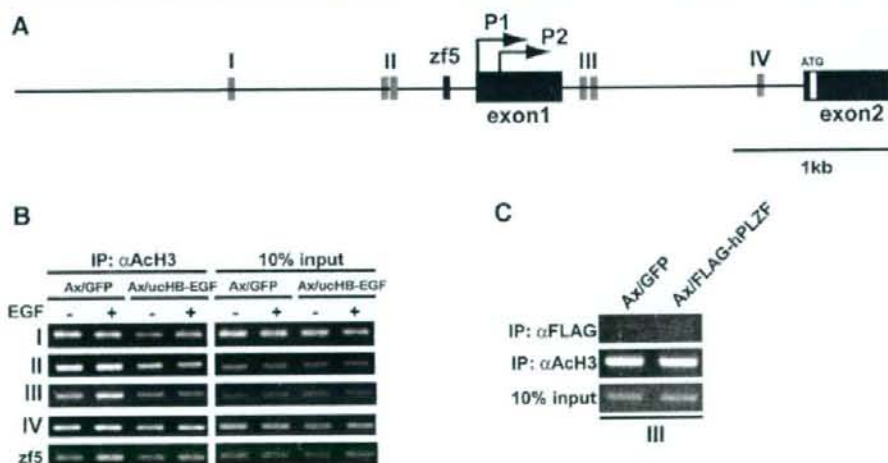

Fig. 7. Inhibition of EGF-induced acetylation of histone H3 at the mouse c-Myc intron I by the uncleavable mutant of proHB-EGF. A: Schematic diagram of the c-Myc promoter, exon I, intron I, and exon II. Gray boxes show the PLZF-binding motif-like sites. The regions including gray boxes are named as regions I, II, III, and IV; zf5 indicates the binding motif of ZF5, a novel c-Myc suppressor; black boxes indicate exons; and P1 and P2 are transcriptional start sites. B: ChIP assay with MEFs infected by adenoviruses including cDNA of GFP or the uncleavable mutant of proHB-EGF, and PLZF (C). All experiments were performed independently in triplicate.

cycle. These results indicate that the shedding event of proHB-EGF is one of the important steps to regulate cell cycle progression, even in the presence of growth factors. Therefore, the present study raises a possibility that cellular behavior involving c-Myc expression is controlled by regulating proteolysis of cell surface proteins and signaling by their cell-associated remnant fragments.

Our current studies indicate that the CTFs of other EGF family members such as amphiregulin, TGF-α, and epiregulin bind to PLZF as well as HB-EGF does (unpublished work, Morimoto and Higashiyama), and that these members share shedding enzymes in some extent (Sahin et al., 2004). The former supports the idea that CTF signaling would be redundant in some members of the EGF family for explaining that the lack of HB-EGF-CTF showed partial inhibition of c-Myc induction by EGF and bFGF. The latter indicates that overexpression of uncleavable proHB-EGF would competitively block the shedding of other members in the EGF family and works as a dominant negative form, explaining that uncleavable proHB-EGF markedly blocked S phase entry of cell cycle induced by EGF and bFGF.

Stimulation of EGF enhanced acetylation of histone H3 at the keratin 16 and c-fos chromatin promoter (Cheung et al., 2000; Wang et al., 2006). We also observed enhanced levels of acetylated histone H3 with EGF treatment in the mouse c-Myc intron I near the boundary of the exon I (Fig. 7B). The activated c-Myc allele in Burkitt's lymphoma is associated with a cluster of somatic mutations within a discrete domain of intron I that define protein recognition sequences, designated as c-Myc intron factors (MIFs) (Zajac-Kaye and Levens, 1990; Tachibana et al., 1993; Yu et al., 1993). The sequence of the intron I in the mouse c-Myc gene is partly homologous to that in the human c-Myc, and this region could also be important in the regulation of the expression of c-Myc in mouse.

PLZF negatively regulates the human cyclin A2 and c-Myc genes (Yeyati et al., 1999; McConnell et al., 2003) and the consensus binding sequence has been identified. We have recently reported that HB-EGF-CTF targets PLZF to de-repress the human cyclin A2 gene (Nanba et al., 2003). It was shown here that shedding of proHB-EGF and sequential production of HB-EGF-CTF affected activation of c-Myc in MEFs, and PLZF may participate in this event. However, over-expression of PLZF did not result in attenuation of acetylation of histone H3 at the intron I region, which includes two similar PLZF-binding motif sites (Fig. 7C). Moreover, we tested the influence of ZF5, a novel regulatory factor for c-Myc expression (Numoto et al., 1993), which has a binding site in the upper region of exon I (Fig. 7A). However, no effects of the uncleavable proHB-EGF mutant were observed at this region in the ChIP assay (Fig. 7B). These results raise the possibility that other C_2H_2 type zinc finger transcriptional repressors with similar features to PLZF might be targeted by HB-EGF-CTF in the expression of mouse c-Myc. This speculation might be supported by two pieces of the following important information. (1) HB-EGF-CTF is able to bind Bcl6, a PLZF-like transcriptional repressor (Kinugasa et al., 2007). (2) PLZF-like repressors (Kruppel-type zinc finger repressors) are well-known gene family showing that active rounds of segmental duplication, involving single genes or larger regions and including both tandem and distributed duplication events, have driven the expansion of this mammalian gene family. Comparisons between the human genes and ZNF loci mined from the draft mouse, dog, and chimpanzee genomes highlighted a substantial level of lineage-specific change. Kruppel-type zinc finger genes are widely expressed and clustered genes are typically not coregulated, indicating that paralogs have evolved to fill roles in many different biological processes in each species (Huntley et al., 2006).
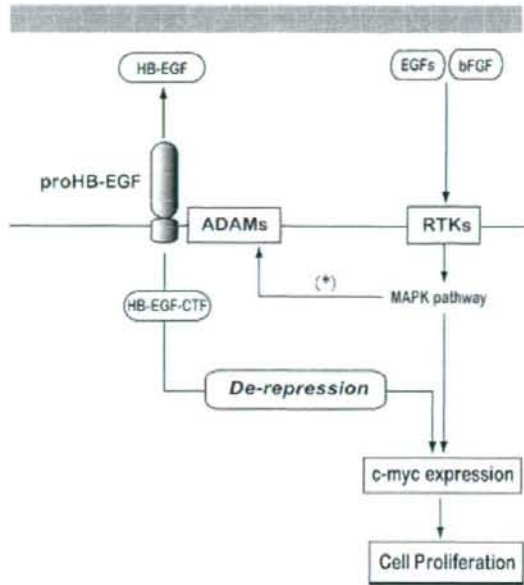

Fig. 8. A schematic diagram for the proposed role of HB-EGF-CTF signaling in c-Myc transcription induced by growth factor receptor activation. (*) Activation of ADAMs by MAPK pathway has already been reported (Gechtman et al., 1999; Umata et al., 2001).

In conclusion, we have shown here that shedding of proHB-EGF induces epigenetic changes in the mouse c-Myc gene, in support of the induction of expression of c-Myc by EGF or bFGF. HB-EGF-CTF may target other transcriptional repressors besides PLZF, and further studies are required to identify the target repressors. We propose a possible model for the mechanism of c-Myc regulation by RTKs in Figure 8.

Literature Cited

Asakura M, Kitakaze M, Takashima S, Liao Y, Ishikura F, Yoshinaka T, Ohmoto H, Node K, Yoshino K, Ishiguro H, Asanuma H, Sanada S, Matsumura Y, Takeda H, Beppu S, Tada M, Hori M, Higashiyama S. 2002. Cardiac hypertrophy is inhibited by antagonism of ADAM12 processing of HB-EGF: Metalloproteinase inhibitors as a new therapy. Nat Med 8:35–40.
Barna M, Hawe N, Niswander L, Pandolfi PP. 2000. Plzf regulates limb and axial skeletal patterning. Nat Genet 25:166–172.
Barone MV, Courtneidge SA. 1995. Myc but not Fos rescue of PDGF signalling block caused by kinase-inactive Src. Nature 378:509–512.
Blobel CP. 2005. ADAMs: Key components in EGFR signalling and development. Nat Rev Mol Cell Biol 6:32–43.

Bouchard C, Thieke K, Maier A, Saffrich R, Hanley-Hyde J, Ansorge W, Reed S, Sicinski P, Bartek J, Eilers M. 1999. Direct induction of cyclin D2 by Myc contributes to cell cycle progression and sequestration of p27. EMBO J 18:5321–5333.

Cheung P, Tanner KG, Cheung WL, Sassone-Corsi P, Denu JM, Allis CD. 2000. Synergistic coupling of histone H3 phosphorylation and acetylation in response to epidermal growth factor stimulation. Mol Cell 5:905–915.

Chiariello M, Marinissen MJ, Gutkind JS. 2001. Regulation of c-myc expression by PDGF through Rho GTPases. Nat Cell Biol 3:580–586.

Dang CV. 1999. c-Myc target genes involved in cell growth, apoptosis, and metabolism. Mol Cell Biol 19:1–11.

Galaktionov K, Chen X, Beach D. 1996. Cdc25 cell-cycle phosphatase as a target of c-myc. Nature 382:511–517.

Gechtman Z, Alonso JL, Raab G, Ingber DE, Klagsbrun M. 1999. The shedding of membrane-anchored heparin-binding epidermal-like growth factor is regulated by the Raf/mitogen-activated protein kinase cascade and by cell adhesion and spreading. J Biol Chem 274:28828–28835.

Goishi K, Higashiyama S, Klagsbrun M, Nakano N, Umata T, Ishikawa M, Mekada E, Taniguchi N. 1995. Phorbol ester induces the rapid processing of cell surface heparin-binding EGF-like growth factor: Conversion from juxtacrine to paracrine growth factor activity. Mol Biol Cell 6:967–980.

Hashimoto K, Higashiyama S, Asada H, Hashimura E, Kobayashi T, Sudo K, Nakagawa T, Damm D, Yoshikawa K, Taniguchi N. 1994. Heparin-binding epidermal growth factor-like growth factor is an autocrine growth factor for human keratinocytes. J Biol Chem 269:20060–20066.

He TC, Sparks AB, Rago C, Hermeking H, Zawel L, da Costa LT, Morin PJ, Vogelstein B, Kinzler KW. 1998. Identification of c-MYC as a target of the APC pathway. Science 281:1509–1512.

Hermeking H, Rago C, Schuhmacher M, Li Q, Barrett JF, Obaya AJ, O'Connell BC, Mateyak MK, Tam W, Kohlhuber F, Dang CV, Sedivy JM, Eick D, Vogelstein B, Kinzler KW. 2000. Identification of CDK4 as a target of c-MYC. Proc Natl Acad Sci USA 97:2229–2234.

Higashiyama S, Nanba D. 2005. ADAM-mediated ectodomain shedding of HB-EGF in receptor cross-talk. Biochim Biophys Acta 1751:110–117.

Huntley S, Baggott DM, Hamilton AT, Tran-Gyamfi M, Yang S, Kim J, Gordon L, Branscomb E, Stubbs L. 2006. A comprehensive catalog of human KRAB-associated zinc finger genes: Insights into the evolutionary history of a large family of transcriptional repressors. Genome Res 16:669–677.

Iwamoto R, Yamazaki S, Asakura M, Takashima S, Hasuwa H, Miyado K, Adachi S, Kitakaze M, Hashimoto K, Raab G, Nanba D, Higashiyama S, Hori M, Klagsbrun M, Mekada E. 2003. Heparin-binding EGF-like growth factor and ErbB signaling is essential for heart function. Proc Natl Acad Sci USA 100:3221–3226.

Kanegae Y, Lee G, Sato Y, Tanaka M, Nakai M, Sakaki T, Sugano S, Saito I. 1995. Efficient gene activation in mammalian cells by using recombinant adenovirus expressing site-specific Cre recombinase. Nucleic Acids Res 23:3816–3821.

Kerkhoff E, Houben R, Loffler S, Troppmair J, Lee JE, Rapp UR. 1998. Regulation of c-myc expression by Ras/Raf signalling. Oncogene 16:211–216.

Kinugasa Y, Hieda M, Hori M, Higashiyama S. 2007. The carboxyl-terminal fragment of Pro-HB-EGF reverses Bcl6-mediated gene repression. J Biol Chem 282:14797–14806.

Leone G, DeGregori J, Sears R, Jakoi L, Nevins JR. 1997. Myc and Ras collaborate in inducing accumulation of active cyclin E/Cdk2 and E2F. Nature 387:422–426.

Mateyak MK, Obaya AJ, Adachi S, Sedivy JM. 1997. Phenotypes of c-Myc-deficient rat fibroblasts isolated by targeted homologous recombination. Cell Growth Differ 8:1039–1048.

McConnell MJ, Chevallier N, Berkofsky-Fessler W, Giltnane JM, Malani RB, Staudt LM, Licht JD. 2003. Growth suppression by acute promyelocytic leukemia-associated protein PLZF is mediated by repression of c-myc expression. Mol Cell Biol 23:9375–9388.

Miyagawa J, Higashiyama S, Kawata S, Inui Y, Tamura S, Yamamoto K, Nishida M, Nakamura T, Yamashita S, Matsuzawa Y, Taniguchi N. 1995. Localization of heparin-binding EGF-like growth factor in the smooth muscle cells and macrophages of human atherosclerotic plaques. J Clin Invest 95:404–411.

Murphy MJ, Wilson A, Trumpp A. 2005. More than just proliferation: Myc function in stem cells. Trends Cell Biol 15:128–137.

Nanba D, Mammoto A, Hashimoto K, Higashiyama S. 2003. Proteolytic release of the carboxy-terminal fragment of proHB-EGF causes nuclear export of PLZF. J Cell Biol 163:489–502.

Niwa H, Yamamura K, Miyazaki J. 1991. Efficient selection for high-expression transfectants with a novel eukaryotic vector. Gene 108:193–199.

Numoto M, Niwa O, Kaplan J, Wong KK, Merrell K, Kamiya K, Yanagihara K, Calame K. 1993. Transcriptional repressor ZF5 identifies a new conserved domain in zinc finger proteins. Nucleic Acids Res 21:3767–3775.

Obaya AJ, Mateyak MK, Sedivy JM. 1999. Mysterious liaisons: The relationship between c-Myc and the cell cycle. Oncogene 18:2934–2941.

Reiss K, Maretzky T, Ludwig A, Tousseyn T, de Strooper B, Hartmann D, Saftig P. 2005. ADAM10 cleavage of N-cadherin and regulation of cell-cell adhesion and beta-catenin nuclear signalling. EMBO J 24:742–752.

Sahin U, Weskamp G, Kelly K, Zhou HM, Higashiyama S, Peschon J, Hartmann D, Saftig P, Blobel CP. 2004. Distinct roles for ADAM10 and ADAM17 in ectodomain shedding of six EGFR ligands. J Cell Biol 164:769–779.

Shirakata Y, Kimura R, Nanba D, Iwamoto R, Tokumaru S, Morimoto C, Yokota K, Nakamura M, Sayama K, Mekada E, Higashiyama S, Hashimoto K. 2005. Heparin-binding EGF-like growth factor accelerates keratinocyte migration and skin wound healing. J Cell Sci 118:2363–2370.

Tachibana K, Takayama N, Matsuo K, Kato S, Yamamoto K, Ohyama K, Umezawa A, Takano T. 1993. Allele-specific activation of the c-myc gene in an atypical Burkitt's lymphoma carrying the t(2;8) chromosomal translocation 250 kb downstream from c-myc. Gene 124:231–237.

Takenobu H, Yamazaki A, Hirata M, Umata T, Mekada E. 2003. The stress- and inflammatory cytokine-induced ectodomain shedding of heparin-binding epidermal growth factor-like growth factor is mediated by p38 MAPK, distinct from the 12-O-tetradecanoylphorbol-13-acetate- and lysophosphatidic acid-induced signaling cascades. J Biol Chem 278:17255–17262.

Tokumaru S, Higashiyama S, Endo T, Nakagawa T, Miyagawa JI, Yamamori K, Hanakawa Y, Ohmoto H, Yoshino K, Shirakata Y, Matsuzawa Y, Hashimoto K, Taniguchi N. 2000. Ectodomain shedding of epidermal growth factor receptor ligands is required for keratinocyte migration in cutaneous wound healing. J Cell Biol 151:209–220.

Umata T, Hirata M, Takahashi T, Ryu F, Shida S, Takahashi Y, Tsuneoka M, Miura Y, Masuda M, Horiguchi Y, Mekada E. 2001. A dual signaling cascade that regulates the ectodomain shedding of heparin-binding epidermal growth factor-like growth factor. J Biol Chem 276:30475–30482.

Wang YN, Chen YJ, Chang WC. 2006. Activation of extracellular signal-regulated kinase signaling by epidermal growth factor mediates c-Jun activation and p300 recruitment in keratin 16 gene expression. Mol Pharmacol 69:85–98.

Yeyati PL, Shaknovich R, Boterashvili S, Li J, Ball HJ, Waxman S, Nason-Burchenal K, Dmitrovsky E, Zelent A, Licht JD. 1999. Leukemia translocation protein PLZF inhibits cell growth and expression of cyclin A. Oncogene 18:925–934.

Yu BW, Ichinose I, Bonham MA, Zajac-Kaye M. 1993. Somatic mutations in c-myc intron 1 cluster in discrete domains that define protein binding sequences. J Biol Chem 268:19586–19592.

Zajac-Kaye M, Levens D. 1990. Phosphorylation-dependent binding of a 138-kDa myc intron factor to a regulatory element in the first intron of the c-myc gene. J Biol Chem 265:4547–4551.

Plasma-membrane-anchored growth factor pro-amphiregulin binds A-type lamin and regulates global transcription

Mayumi Isokane[1,2], Miki Hieda[1], Satoshi Hirakawa[3], Masachika Shudou[4], Koichi Nakashiro[2], Koji Hashimoto[3], Hiroyuki Hamakawa[2] and Shigeki Higashiyama[1,5,*]

[1]Department of Biochemistry and Molecular Genetics, [2]Department of Oral and Maxillofacial Surgery, [3]Department of Dermatology, [4]Department of Bioscience, INCS and [5]Protein Network Laboratory, CEREM, Ehime University Graduate School of Medicine, Toon, Ehime 791-0295, Japan
*Author for correspondence (e-mail: shigeki@m.ehime-u.ac.jp)

Summary

Amphiregulin (AR), a member of the EGF family, is synthesized as a type I transmembrane protein precursor (proAR) and expressed on the cell surface. Shedding of proAR yields a transmembrane-cytoplasmic fragment (AR-CTF), as well as a soluble AR. Here we demonstrate that the proAR-shedding stimuli trigger endocytosis of both AR-CTF and un-shed proAR. ProAR translocates from the plasma membrane to the inner nuclear membrane, whereas AR-CTF is translocated to the lysosome via retrograde membrane trafficking. Nuclear envelope localization of proAR involves truncation of the C-terminus, which subsequently activates the ER-retrieval signal. The truncated form of proAR interacts with A-type lamin and is retained at the inner nuclear membrane. Heterochromatin formation is then induced and global transcription is transiently suppressed. This study gives new insight into epigenetic chromatin organization in mammalian cells: a plasma-membrane-anchored growth factor is targeted to the inner nuclear membrane where it participates in dynamic chromatin organization and control of transcription.

Supplementary material available online at
http://jcs.biologists.org/cgi/content/full/121/21/3608/DC1

Key words: Amphiregulin, Heterochromatin, Inner nuclear membrane, Lamin, RNA polymerase II transcription

Introduction

Over the 25 years, research on the epidermal growth factor (EGF) family and EGF receptors has provided numerous key insights into development, homeostasis and disease. The EGF family comprises 13 members, all of which are synthesized as type I transmembrane protein precursors and are subsequently expressed on the plasma membrane (Higashiyama et al., 2008). These transmembrane forms serve not only as juxtacrine factors (Anklesaria et al., 1990; Higashiyama et al., 1995; Singh and Harris, 2005), but also as intermediaries of EGF-receptor (EGFR) transactivation (Blobel, 2005; Higashiyama et al., 2008), which can play a major role in signaling by G-protein-coupled receptors (GPCRs), cytokine receptors and receptor tyrosine kinases (Rozengurt, 2007). Transactivation of EGFRs is mediated, in many cases, by soluble forms of EGF-family ligands, which are cleaved from their membrane-anchored forms (proforms) in a process termed 'ectodomain shedding' (Higashiyama et al., 2008).

The precursor of amphiregulin (proAR), which is a member of the EGF family, shares overall structural homology with other members of the EGF family. ProAR shedding from the cell surface involves a disintegrin and metalloprotease 17 (ADAM17) (also known as tumor necrosis factor-α converting enzyme or TACE) (Sahin et al., 2004; Hinkle et al., 2004). Ectodomain shedding of proAR is induced by stimulants, such as 12-O-tetradecanoylphorbol-13-acetate (TPA). Activation of proAR shedding produces a plasma-membrane-anchored remnant C-terminal fragment (AR-CTF) and leaves a significant amount of un-shed proAR on the cell surface (Tokumaru et al., 2000). The fate of AR-CTF and proAR post-activation of the shedding process remains unclear. Recently we reported that ectodomain shedding of proHB-EGF, another member of the EGF family, evokes two independent signaling pathways: EGFR signaling induced by the shed extracellular domain and signaling driven by a remnant peptide comprised of the transmembrane and cytoplasmic domains (Nanba et al., 2003). Cytoplasmic domain signaling is mediated by interaction with at least two transcriptional repressors, known as promyelocytic leukemia zinc finger (PLZF) and B-cell lymphoma 6 (Bcl6), reversing PLZF-and Bcl6-mediated gene repression (Nanba et al., 2003; Kinugasa et al., 2007). We have also demonstrated translocation of proHB-EGF from the cell surface to the inner nuclear membrane (INM), where binding to the transcriptional repressors probably occurs (Hieda et al., 2008).

The nuclear envelope consists of the INM and an outer nuclear membrane (ONM), which are joined at the nuclear pore membrane. The ONM is structurally continuous with the peripheral ER. The nuclear lamina is a scaffold-like network of protein filaments underneath the INM. The scaffold consists primarily of type V intermediate filament proteins: lamin A/C, which is encoded by a single gene (LMNA) and expressed only in differentiated cells; and lamin B, which is encoded by two human genes (LMNB1 and LMNB2) and found in nearly all somatic cells (Vlcek et al., 2001; Gruenbaum et al., 2005). Lamins support a broad range of functions through interaction with

various proteins, including INM proteins, chromatin, components of the RNA-polymerase-II-dependent transcription complex, and DNA replication complexes, suggesting that lamins are involved not only in nuclear structures, but also in DNA replication and gene expression (Spann et al., 1997; Spann et al., 2002; Goldman et al., 2002; Schirmer et al., 2003). Furthermore, it has been reported that mutations in *LMNA* or in the A-type lamin-binding proteins cause various diseases termed laminopathies. To date, there are about 50 known mutations in *LMNA* that cause laminopathies. These diseases affect striated muscle (Emery-Dreifuss muscular dystrophy or EDMD), cardiac muscle (dilated

cardiomyopathy CMD1A), limb-girdle muscle and neurons (Charcot-Marie-Tooth disorder AR-CMT2B1), adipose tissue (familial partial lipodystrophy FPLD), and adipocytes and bone (mandibuloacral dysplasia MAD) (Mounkes et al., 2003).

The results of the present study demonstrate that (1) AR-CTF and un-shed proAR are internalized in response to ectodomain-shedding stimuli and then translocated to lysosomes and ER or nuclear envelope, respectively; (2) un-shed proAR is subsequently translocated to the INM where it is retained; and (3) the INM-targeted un-shed proAR induces heterochromatin formation and suppression of global transcription.
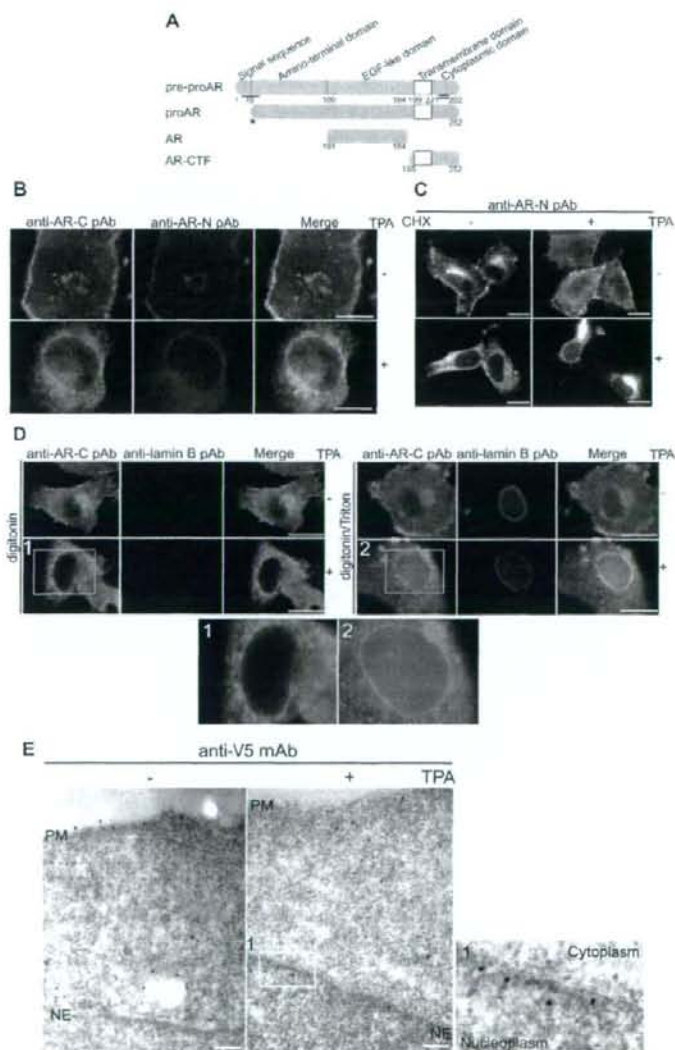

Fig. 1. ProAR translocates from the plasma membrane to the inner nuclear membrane. (A) Schematic representation of human *AREG* gene products. The AR coding region is translated as a precursor form (pre-proAR) with five structural domains consisting of predicted 252 amino acids (Plowman et al., 1990). The signal sequence is trimmed off, and the resulting protein is expressed on the plasma membrane as proAR whose N-terminal sequence is not yet determined (*). In response to various stimuli, proAR is shed at the juxtamembrane domain, resulting in the production of AR and AR-CTF. Anti-AR-N and anti-AR-C pAbs specifically recognize the extracellular and the cytoplasmic domains of proAR, respectively. The single line is the epitope region of anti-AR-N pAb, and double line is that of anti-AR-C pAb. (B) HeLa cells were transfected with a full-length *AREG* plasmid, then incubated with or without TPA. Cells were immunostained with anti-AR-N or anti-AR-C pAb. (C) HeLa cells transiently expressing *AREG* were incubated with 20 μg/ml cycloheximide for 60 minutes. The cells were then treated with TPA and immunostained with anti-AR-N pAb. (D) HeLa cells transiently expressing *AREG* were permeabilized with digitonin and then fixed. The cells were re-permeabilized with (left panels) or without (right panels) Triton X-100, and immunostained with anti-AR-C (green) or/and anti-lamin B (red) pAbs. The lower panels are high magnification images of the boxed regions labelled 1 and 2. Scale bars: 5 μm. (E) Ultra-thin sections were stained with anti-V5 mAb and 15 nm gold-conjugated secondary antibodies. Right panel, without TPA; middle panel, with TPA; left panel, high magnification image of boxed region in middle panel. PM, plasma membrane; NE, nuclear envelope. Scale bars: 200 nm.

Results
Un-shed proAR and AR-CTF are targeted to the INM and lysosome, respectively

Amphiregulin (AR; official symbol AREG) is synthesized as a type I transmembrane protein (pre-proAR) and is expressed on the plasma membrane as a 25-50 kDa precursor (proAR). ProAR contains an extracellular EGF-like domain, a transmembrane segment and a short cytoplasmic tail (Fig. 1A). ProAR is cleaved at the juxtamembrane domain via metalloprotease activation, yielding a soluble AR and a C-terminal fragment that contains transmembrane and cytoplasmic segments (AR-CTF). HeLa cells transiently transfected with *AREG* were immunostained with two polyclonal antibodies, anti-AR-N and anti-AR-C, which recognize the extracellular and cytoplasmic domains of proAR, respectively. ProAR-positive staining was visualized at the plasma membrane and the perinuclear organelles under steady-state conditions (Fig. 1B, upper panels). The perinuclear signal colocalized with the Golgi complex marker protein, GM130 (data not shown). In the presence of a shedding stimulus (TPA), the anti-AR-N and anti-AR-C signals were both observed in the reticular meshwork, evidently in the ER and nuclear envelope (Fig. 1B, lower). This result suggests translocation of un-shed proAR from the plasma membrane to the

ER or nuclear envelope. To verify that the proAR in the reticular meshwork was not newly synthesized protein, de novo synthesis was blocked with cycloheximide. In the presence of cycloheximide, the proAR signal in the Golgi disappeared; however, proAR staining was evident at the plasma membrane and shifted to the ER and nuclear envelope after TPA stimulation (Fig. 1C). Thus, proAR on the plasma membrane translocates to the ER and nuclear envelope.

If proAR is targeted to the INM, cytoplasmic domains face the nucleoplasm and can physically interact with proteins localized inside the nucleus. Thus, it is crucial to determine whether nuclear-envelope-targeted proAR localizes to the ONM or to the INM. We took advantage of the fact that low concentrations of digitonin selectively permeabilize the plasma membrane, but leave the nuclear membrane intact (Adam et al., 1990). Digitonin treatment allowed detection of anti-AR-C signal at the plasma membrane and Golgi without TPA treatment and at the ER after TPA treatment. Lamin B signal was not detected, whether cells were treated with TPA or not. Lamins form a network of filaments underlying the INM and require Triton X-100 permeabilization for antibody detection. After Triton X-100 treatment and digitonin permeabilization, an AR-C signal was detected at the nuclear
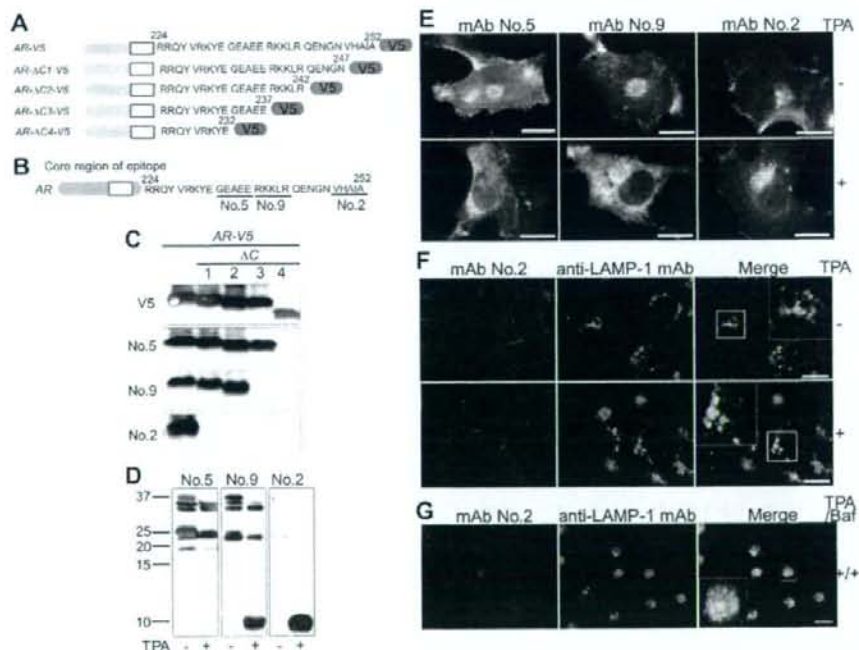

Fig. 2. ProAR is targeted to the nuclear envelope. (A) Schematic presentation of AR deletion mutants. All constructs (AR-V5, AR-ΔC1-V5, AR-ΔC2-V5, AR-ΔC3-V5 and AR-ΔC4-V5) were V5-tagged at the C-terminus. (B) Three monoclonal antibodies mAb2, mAb5 and mAb9 against the cytoplasmic domain of proAR were established. The core epitope region for each antibody is underlined. (C) Total lysates of HeLa cells expressing AR-V5 or AR-ΔC-V5 mutants were analyzed by immunoblotting with the three mAbs. An anti-V5 mAb was used as a positive control. (D) Lysates of HeLa cells expressing wild-type *AREG* were immunoblotted with anti-AR-C mAbs. (E and F) HeLa cells transiently expressing wild-type *AREG* were incubated with or without TPA for 30 minutes and immunostained with the anti-AR-C mAbs (E) or mAb2 and anti-LAMP-1 mAbs (F). (G) HeLa cells transiently expressing wild-type *AREG* were treated with 50 nM Bafilomycin (Baf) for 60 minutes and incubated with TPA in the presence of Baf. The cells were then immunostained with mAb2 and anti-LAMP-1 mAb. Scale bars: 5 μm.

envelope in response to TPA treatment and a lamin B signal was evident, which was independent of TPA treatment (Fig. 1D). The detection of AR-C signal after Triton X-100 and digitonin treatment indicated that the cytoplasmic domain of proAR was exposed into the nucleoplasm after TPA stimulation (Fig. 1D, lower panel). These results suggest that the un-shed proAR could be targeted to the INM after TPA treatment. Next, we detected proAR at the nucleoplasmic face of the nuclear envelope in TPA-treated cells using immunoelectron microscopy (Fig. 1E). We conclude that un-shed proAR can localize at the INM upon shedding stimuli.

To identify the functional domain(s) involved in intracellular localization, we prepared monoclonal antibodies (mAbs) against the cytoplasmic domain of proAR, and obtained three clones (termed mAb2, mAb5 and mAb9) that recognized distinct epitopes (Fig. 2B). To identify the epitope region, we used the C-terminal deletion mutants of AR (Fig. 2A). The ability of mAb2, mAb9 and mAb5 to bind proAR was abrogated by deleting the C-terminal 5, 15 and 20 amino acids of proAR, respectively (Fig. 2C). In western blot analysis, mAb5 efficiently recognized proAR, but not the ~10 kDa AR-CTF (Fig. 2D). The mAb9 bound both proAR and AR-CTF, whereas mAb2 preferentially bound AR-CTF (Fig. 2D). Because AR-CTF encompasses the mAb5 epitope region, these results suggest that the mAb5 epitope region might be modified in AR-CTF. Immunofluorescent microscopy revealed that all mAbs stained the plasma membrane and the Golgi complex in the absence of TPA, although the signal from mAb2 was weaker than that from the other antibodies (Fig. 2E, upper panel). After TPA treatment, mAb5 and mAb9 detected proAR localized in the ER and nuclear envelope (Fig. 2E, lower panel), which was also detected with anti-AR-N pAbs (data not shown). However, mAb2 did not detect proAR in the ER and nuclear envelope (Fig. 2E, lower panel), suggesting that the mAb2 epitope might be masked or removed in proAR localized in this region. Interestingly, organelles detected by mAb2 were partially recognized by a mAb that was specific for LAMP-1, which is a lysosome marker protein (Fig. 2F), but were not recognized by anti-AR-N pAb (data not shown). In the presence of bafilomycin (Baf), which inhibits the lysosomal proton pump, thereby suppressing membrane trafficking through lysosomes, the signal for mAb2 significantly colocalized with the LAMP-1 signal (Fig. 2G).

These results imply that un-shed proAR targeted to the ER and nuclear envelope might be modified at the C-terminus (i.e. in the

mAb2 epitope region), whereas AR-CTF accumulates in lysosomes. We speculate that masking of the epitope recognized by mAb5 in AR-CTF might signal lysosome targeting. Thus, we focused hereafter on the localization and function of un-shed proAR.
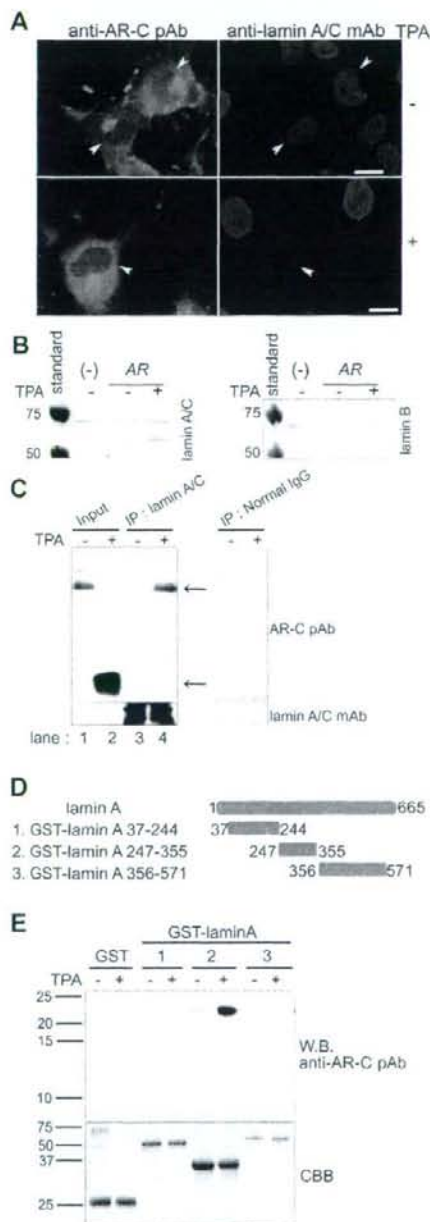

Fig. 3. ProAR interacts with A-type lamin. (A) HeLa cells transiently expressing wild-type *AREG* were incubated with or without TPA. Cells were stained with anti-AR-C pAb and anti-lamin A/C mAb. Arrowheads indicate *AREG*-expressing cells. Scale bars: 5 μm. (B) Lysates of HeLa cells transiently transfected with or without wild-type *AREG* and treated with TPA for 60 minutes, were subjected to immunoblotting using anti-lamin A/C mAb (left) or anti-lamin B pAb (right). The left lanes show standard proteins. (C) HeLa cells transiently expressing wild-type *AREG* were incubated with or without TPA for 60 minutes. The cell lysates were subjected to immunoblotting with an anti-AR-C pAb (lane 1 and lane 2). The cell lysates were immunoprecipitated with an anti-lamin A/C mAb or normal mouse IgG, followed by western blotting using anti-AR-C pAb and anti-lamin A/C mAb. Arrows indicate the molecular mass of lamin A/C-interacted (upper) and AR-CTF (lower). (D) Schematic representation of GST-fused lamin A deletion mutants. (E) The cell lysates from cells transiently expressing wild-type *AREG* were incubated with GST or GST-lamin A derivatives, which were pulled down by glutathione-Sepharose beads. Bound proteins were analyzed by western blotting using the anti-AR-C pAb (upper panel). GST fusion proteins were analyzed by SDS-PAGE and stained with CBB (lower panel).

Un-shed proAR interacts with A-type lamin

Some proteins are tethered to the INM because of interactions with INM-resident proteins (Holmer and Worman, 2001). The intensity of anti-lamin A/C mAb staining decreased in AR-expressing cells after TPA treatment (Fig. 3A), even though lamin protein levels remained unchanged (Fig. 3B). This observation suggests a physical interaction between AR and A-type lamin. Immunoprecipitation was used to examine this possibility. Un-shed proAR, but not AR-CTF, co-precipitated with an anti-lamin A/C mAb; TPA treatment markedly enhanced binding between AR and lamin A/C (Fig. 3C). Precipitated un-shed proAR migrated slightly faster than proAR, suggesting that it was smaller than proAR (Fig. 3C). Neither normal mouse IgG nor anti-lamin B pAb immunoprecipitated un-shed proAR (Fig. 3C and supplementary material Fig. S1A). GST-tagged deletion mutants of lamin A pulled down proAR from the total cell lysate. This result demonstrates that a sequence within the lamin A

region spanning residues 247-355 (shared with lamin C) is essential for the interaction with AR (Fig. 3D,E).

Next, siRNA duplexes targeting lamin A/C were used to examine the lamin A/C requirement for INM localization of un-shed proAR. Transfection with siRNA duplexes resulted in a marked and specific reduction in levels of lamin A/C protein (Fig. 4A). Lamin A/C downregulation abrogated localization of un-shed proAR in the nuclear envelope, but did not affect accumulation of proAR in the perinuclear structure in the presence of TPA (Fig. 4B). Control siRNA or knockdown of lamin B did not affect nuclear envelope targeting of proAR (Fig. 4B and supplementary material Fig. S1B). Thus, it was concluded that lamin A/C is essential for localization of proAR to the nuclear envelope.

Un-shed proAR that interacts with A-type lamin is truncated at the C-terminus

Because the proAR that interacted with lamin A/C migrated slightly faster than proAR (Fig. 3C) and mAb2 did not recognize the proAR targeted to the ER and nuclear envelope in immunofluorescence studies (Fig. 2E), we hypothesized that the epitope recognized by mAb2 might be removed from INM-localized proAR. This hypothesis was tested by immunoprecipitation studies. As shown in Fig. 5A, mAb2 was unable to detect proAR that had been co-
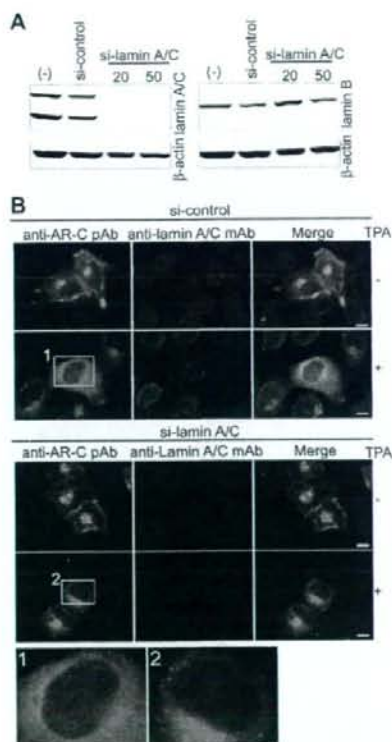

Fig. 4. A-type lamin is essential for targeting of proAR to the nuclear envelope. (A) HeLa cells were transfected with 20 nM or 50 nM of lamin A/C-targeting duplex siRNA (si-lamin A/C) or control siRNA (si-control). After 72 hours, the cells lysates were analyzed by western blotting with anti-lamin A/C mAb or anti-lamin B pAb. (B) HeLa cells were transfected twice: first with 20 nM of control siRNA (upper) or lamin A/C-siRNA (lower); and, after 48 hours, with wild-type *AREG* plasmid. After 24 hours, cells were stimulated with or without TPA, and then fixed. Cells were stained with anti-AR-C pAb and anti-lamin A/C mAb. The lower panels (1 and 2) are high magnification images of the boxed areas above. Scale bars: 5 μm.
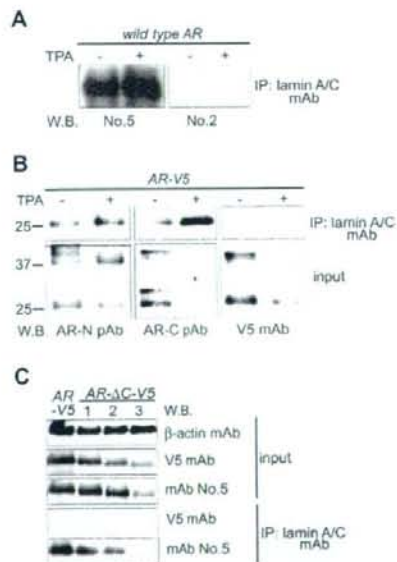

Fig. 5. Un-shed proAR that interacts with A-type lamin is truncated at the C-terminus. (A) HeLa cells transiently expressing wild type *AREG* were incubated with or without TPA. Cell lysates were immunoprecipitated with anti-lamin A/C mAb and analyzed by western blot using the mAb5 and mAb2. (B) HeLa cells transiently expressing AR-V5 were incubated with or without TPA. Cell lysates were immunoprecipitated with anti-lamin A/C mAb. Cell lysates (upper) and precipitated proteins (lower) were analyzed with indicated mAbs. (C) Cell lysates of HeLa cells expressing AR-V5, AR-ΔC1-V5 (lane 1), AR-ΔC2-V5 (lane 2) or AR-ΔC3-V5 (lane 3) were immunoprecipitated with anti-lamin A/C mAb. Cell lysates and precipitated proteins were analyzed with anti-β-actin, anti-V5 mAb or mAb5.

precipitated with lamin A/C. This result implies that proAR that interacts with lamin A/C lacks the portion of the C-terminus containing the epitope recognized by mAb2. We examined this possibility in greater detail using C-terminal-V5-tagged proAR (Fig. 2A). Anti-AR-N and anti-AR-C pAbs recognized the co-precipitated proAR, but an anti-V5 mAb did not (Fig. 5B). These results demonstrate that the proAR that interacts with lamin A/C did not contain the V5 tag. Furthermore, two deletion mutants, AR-ΔC1-V5 and AR-ΔC2-V5 (Fig. 2A) were co-precipitated with an anti-lamin A/C mAb. Thus, the C-terminal 10 amino acids are not required for lamin A/C binding (Fig. 5C). All proAR proteins co-immunoprecipitated with anti-lamin A/C mAb were the same size (Fig. 5C, bottom panel) and were not detected using an anti-V5 mAb (Fig. 5C, second panel from the bottom). Taken together, these results show that proAR interacting with lamin A/C is truncated at the C-terminus. Mass spectrometric analysis of proAR co-immunoprecipitated with anti-lamin A/C mAb was performed to determine the cleavage site. However, the lysine- and arginine-rich sequence in the cytoplasmic domain made it difficult to identify the enzymatic digest products.

Lys239 and Lys240 in the cytoplasmic domain of proAR are essential for targeting to the nuclear envelope

Most ER-resident type I transmembrane proteins have the ER-retention signal, K-K-x-x (x is any amino acid), at the C-terminus (Nilsson et al., 1989; Jackson et al., 1990). Interestingly, the K-K-x-x motif exists in the cytoplasmic domain of proAR, although it is not exposed at the distal terminus (Fig. 6A). When Ala residues were substituted for Lys239 and Lys240 (AR-m2) in proAR, targeting to the nuclear envelope did not occur, even after TPA treatment. Instead, the proAR-m2 accumulated in the perinuclear region colocalized with TGN46, a trans-Golgi marker (Fig. 6B). These results indicate that Lys239 and/or Lys240 are essential for ER targeting. To analyze the mechanism of proAR targeting to the ER, a V5 epitope tag was inserted into proAR just downstream from the transmembrane domains (AR-V5-C). The V5-tag insertion had no effect on localization of proAR to the plasma membrane and Golgi under steady state conditions. Likewise, insertion of the V5 tag did not affect targeting to the nuclear envelope in response to TPA stimulation (Fig. 6C,D). Notably, deletion of 10 residues at the C-terminus (AR-V5-ΔC10) to expose $_{239}$KKLR$_{242}$-induced localization of proAR to the ER and nuclear envelope, even in the absence of TPA treatment (Fig. 6D). However anti-lamin A/C mAb staining was only slightly reduced in AR-V5-ΔC10 transfectants (compare Fig. 6E and Fig. 3A) and the interaction with lamin A/C was very weak (Fig. 6F). We then created an 11-residue deletion mutant (AR-V5-ΔC11), which exposed $_{238}$RKKL$_{241}$ at the C-terminus, and observed ER and nuclear envelope localization in the steady state. Anti-lamin A/C mAb staining was markedly reduced and a significant interaction with lamin A/C was observed (Fig. 6E,F). In addition, a 12-residue deletion mutant of
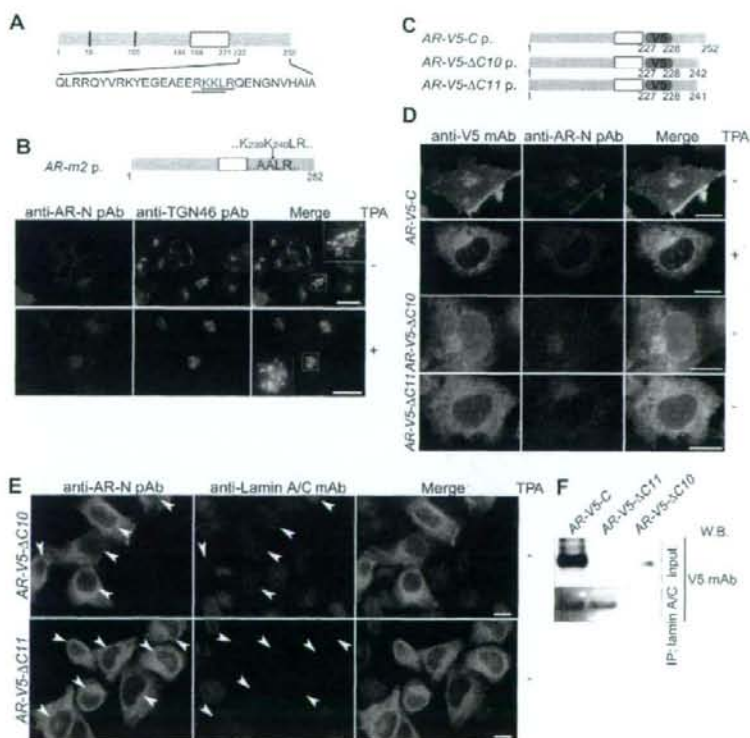

Fig. 6. Lysine239 and/or lysine240 in the cytoplasmic domain of proAR are essential for targeting to the nuclear envelope. (A) Amino acid sequence of the cytoplasmic domain of proAR. (B) Schematic representation of mutations in K239 and K240 in the cytoplasmic domain (AR-m2). AR-m2 p indicates AR-m2 precursor protein. HeLa cells transfected with AR-m2 were incubated with or without TPA and immunostained with anti-AR-N pAb (red) and anti-TGN46 pAb (green). (C) Schematic representation of V5-tag inserted AR and its deletion mutants. AR-V5-C p, AR-V5-ΔC10 p and AR-V5-ΔC11 p indicate precursor proteins. (D,E) HeLa cells transiently expressing AR-V5-C, AR-V5-ΔC10 or AR-V5-ΔC11 were incubated with or without TPA, then immunostained with anti-V5 mAb and anti-AR-N pAb (D) or with anti-AR-N pAb and anti-lamin A/C mAb (E). Arrowheads indicate AR-expressing cells. (F) Cell lysates of HeLa cells expressing AR-V-C5, AR-V5-ΔC10 or AR-V5-ΔC11 were immunoprecipitated with anti-lamin A/C mAb. Cell lysates (upper) and precipitated proteins (lower) were analyzed with anti-V5 mAb. Scale bars: 5 μm.

proAR (AR-V5-ΔC12), in which $_{237}$ERKK$_{240}$ was exposed at the C-terminus, did not localize to the ER and nuclear envelope (data not shown). These results indicate that $_{239}$KKLR$_{242}$ and $_{238}$RKKL$_{241}$ in the cytoplasmic domain of proAR function as ER-retention signals when exposed at the distal C-terminus, but the activity of AR-V5-ΔC11 seems to be equivalent to that of the wild type, unlike AR-V5-ΔC10. Thus, the exact cleavage site remains to be identified. Although it is plausible that lamin-A/C-interacting proAR might lack 11 amino acids at the C-terminus, resulting in ER and nuclear envelope targeting.

Nuclear-envelope-targeted proAR masks a lamin A/C epitope in dense heterochromatin

The intensity of lamin A/C mAb staining was decreased in cells expressing nuclear-envelope-targeted proAR, even though A-type lamin protein levels remained unchanged (Fig. 3A,B) and anti-lamin

A/C pAb stained these cells (data not shown). Epitope masking of lamin A/C in immunofluorescence studies as a result of interactions with chromatin and other proteins is a well known phenomenon (Hozák et al., 1995; Dyer et al., 1997; Kumaran et al., 2002; Markiewicz et al., 2005). To explore epitope masking due to lamin interactions with chromatin or other proteins, AR-expressing cells were treated with DNase I, NaCl and/or Triton X-100 before fixation (Markiewicz et al., 2005). Triton X-100 and/or NaCl extraction had no affect on lamin A/C staining. When cells were treated with Triton X-100, NaCl and DNase I, the lamin A/C signal was apparently recovered (Fig. 7A). We tried to extract DNA using NaCl and DNase I; however, the efficiency of chromosomal DNA extraction, judged by Hoechst 33342 staining, was too low (data not shown). These results suggest that epitope masking occurs because of physical associations between lamin and chromatin. Intriguingly, the epitope for the anti-lamin A/C mAb is located in a region spanning amino residues 356-571 (data not shown), which corresponds to the chromatin-binding domain (Zastrow et al., 2004).

Nuclear-envelope-targeted proAR induces diverse heterochromatin assembly

To verify the physiological role of nuclear-envelope-targeted AR, we focused on the proAR-lamin-A/C interaction. We observed that nuclear envelope targeting of proAR induced heterochromatinization, as evidenced by strong staining with Hoechst 33342 (Fig. 7B). Overexpression of other INM proteins (e.g. HB-EGF and lap2β) did not induce this heterochromatinization (supplementary material Fig. S3). Higher-order assembly of chromatin is thought to be largely determined by post-translational methylation of histone tails at H3 Lys9 (H3K9), which is essential for localization of HP1. As expected, it could be observed that Hoechst 33342 staining was accompanied by an increase in trimethylation of H3K9 (H3K9me3) in cells with nuclear-envelope-targeted proAR. Moreover, the heterochromatin protein, HP1β colocalized with Hoechst 33342 staining in these cells (Fig. 7B). Western blot analysis confirmed the relative increase of H3K9me3 in cells transiently expressing proAR after TPA treatment and cells expressing AR-Δ11 without TPA treatment (Fig. 7C).

Nuclear-envelope-localizing proAR suppresses global transcription

Heterochromatin can propagate, and thereby influence, gene expression in a region-specific
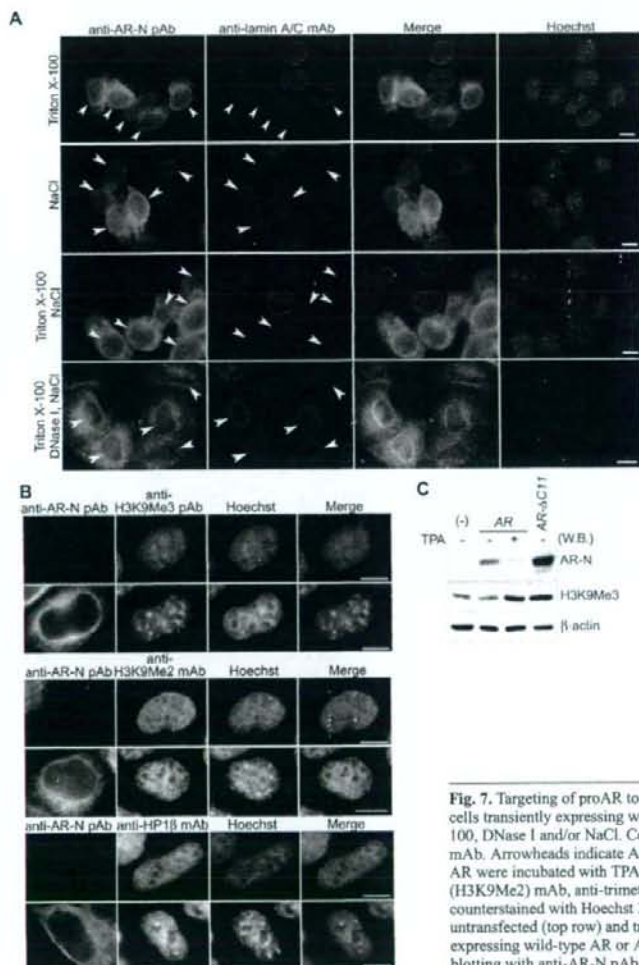

Fig. 7. Targeting of proAR to the nuclear envelope causes heterochromatin assembly. (A) HeLa cells transiently expressing wild-type AR were incubated with TPA and treated with Triton X-100, DNase I and/or NaCl. Cells were then stained with anti-AR-N pAb and anti-lamin A/C mAb. Arrowheads indicate AR-expressing cells. (B) HeLa cells transiently expressing wild-type AR were incubated with TPA and then stained with anti-AR-N pAb, anti-dimethylated H3K9 (H3K9Me2) mAb, anti-trimethylated H3K9 (H3K9Me3) pAb and anti-HP1b pAb. Cells were counterstained with Hoechst 33342. Each panel shows representative cells that are untransfected (top row) and transfected (bottom row). (C) Cell lysates of HeLa cells transiently expressing wild-type AR or AR-ΔC11 treated with or without TPA were analyzed by western blotting with anti-AR-N pAb, anti-H3K9Me3 mAb and anti-β-actin mAb. Scale bars: 5 μm.

and sequence-independent manner. When heterochromatin spreads across domains, it generally causes epigenetic repression of nearby sequences. Thus, the diverse heterochromatin formation

A

B Quantification of Br-U intensity in the nucleus

C

Fig. 8. Targeting of proAR to the nuclear envelope induces transient suppression of global transcription. (A,C) 5 mM Br-U was added in the presence or absence of TPA to the culture medium of HeLa cells transiently expressing AR-V5-C (A), AR-V5-ΔC10 or AR-V5-ΔC11 (C) followed by a 30 minute incubation. Cells were fixed and immunostained with anti-BrdU mAb, anti-V5 mAb and Hoechst 33342. Asterisks indicate AR-expressing cells. (B) HeLa cells transiently expressing AR-V5-C were incubated with or without TPA for 30 minutes and re-grown in fresh medium for the duration indicated. 5 mM Br-U was added to the culture medium 30 minutes prior to fixation. After fixation, Br-U incorporated in mRNA was stained with anti-BrdU mAb and fluorescent intensity in the AR-expressing cells was quantified (n=200). Statistical analysis was carried out as described in Materials and Methods. Scale bars: 5 μm.

in AR-expressing cells prompted us to examine global transcriptional activity. Synthesis of RNA transcripts was monitored using incorporation of bromo-uridine (Br-U) (Iborra et al., 1998). This analogue does not affect activity of the major polymerizing enzyme RNA polymerase II. Newly synthesized Br-U-labeled RNA (Br-RNA), with the exception of nucleolar RNA, can be detected with anti-BrdU mAb after formaldehyde fixation (Koberna et al., 1999). In the present study, newly synthesized RNA was dramatically reduced in cells with nuclear-envelope-targeted proAR, even though Br-RNA intensity in untransfected cells was not affected by TPA treatment (Fig. 8A) and overexpressed HB-EGF or lap2β (supplementary material Fig. S2B,C). To exclude the possibility that reduced transcriptional activity was due to cell death, cell proliferation and Br-U incorporation were monitored for 24 hours. Quantitative analysis showed that global transcription was dramatically suppressed after exposure to a shedding stimulus by approximately 80% for up to 4 hours, after which time transcription was recovered within 24 hours. Statistical analysis showed that there are significant differences between the presence and absence of shedding stimuli. Interestingly, ectopic expression of AR-V5-ΔC11, which is localized to the nuclear envelope in the absence of shedding stimuli suppressed global transcription without TPA treatment (Fig. 8C). Moreover the global transcription in the AR-V5-C-expressing cells in which lamin A/C was knocked down was not affected (supplementary material Fig. S3). These results indicate that proAR-lamin-A/C interaction induces heterochromatinization and global transcriptional repression. The total pool of hyperphosphorylated and hypophosphorylated largest RNA polymerase II subunit was unchanged in western blot analysis (data not shown). Heterochromatin assembly is commonly associated with large-scale chromatin condensation and reorganization of the nuclear domain. Both these conditions reduce the accessibility of transcription machinery to heterochromatic loci. Thus, it was concluded that nuclear-envelope-targeting of proAR suppressed the global transcription. This might be due to reduced accessibility rather than regulation of transcriptional machinery.
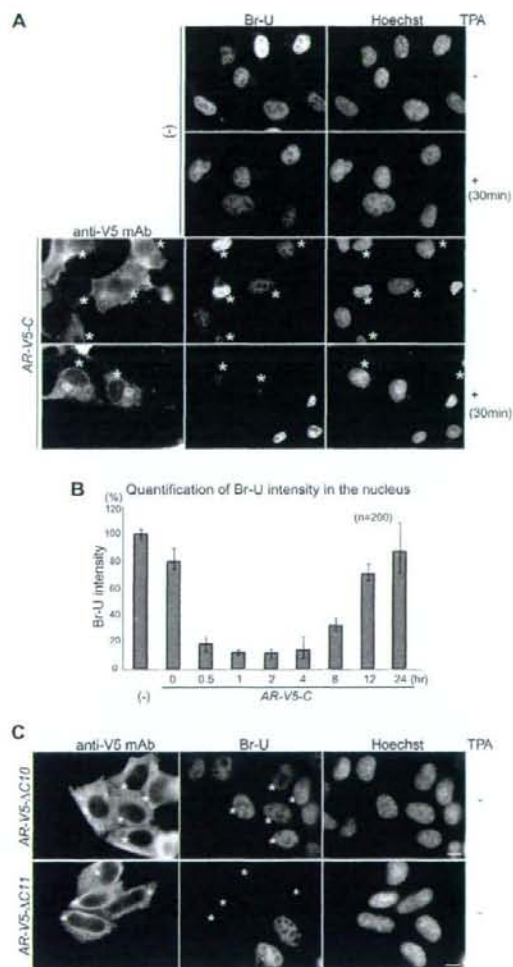
Discussion

A model of proAR targeting from the plasma membrane to the inner nuclear membrane

The efficiency of proAR-ectodomain shedding is moderate (Tokumaru et al., 2000), resulting in the production of AR, AR-CTF and un-shed proAR. Herein, we provide evidence that proAR is translocated from the plasma membrane to the INM, where it is tethered by interaction with A-type lamin. Based on our results, we propose a model for this retrograde transport pathway, as shown in Fig. 9. First, proAR is primarily localized at the plasma membrane. Shedding stimuli induce internalization of both AR-CTF and un-shed proAR. Internalized AR-CTF and un-shed proAR are then targeted to different destinations, the lysosome and INM, respectively, suggesting different functions. The molecular mechanisms of the differential intracellular sorting remain unknown, but two types of modifications in the cytoplasmic region may be key events: epitope masking and truncation of the C-terminus. Masking of the epitope recognized by mAb5 in AR-CTF was suggested by the observation that this antibody was barely able to detect AR-CTF, whereas mAb2 showed a strong signal. We speculate that this masking modification might act as a lysosomal-sorting signal. AR-CTF is likely to have a full-length cytoplasmic tail given the fact that it can bind to mAb2, even though
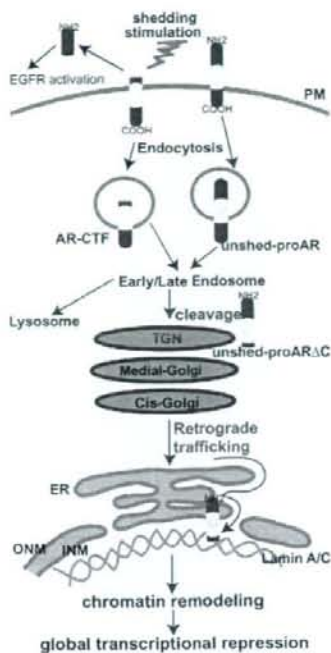
Fig. 9. Schematic representation of proAR intracellular trafficking. Without TPA stimulation, proAR primarily localizes at the plasma membrane. TPA induces partial proAR-ectodomain shedding, resulting in the production of a soluble growth factor (AR) and a C-terminal fragment (AR-CTF). In addition, TPA causes the endocytosis of both AR-CTF and the residual un-shed proAR. AR-CTF then translocates to the lysosome (black arrow) and un-shed proAR traffics to the INM (red arrow). During translocation to the INM, proAR is truncated at the C-terminus, and targeted to the ER. Subsequently ER-localized proAR diffuses or is actively transported to the INM, where it is tethered via interaction with A-type lamin and downregulates global transcription. PM, plasma membrane.

INM-targeted proAR is truncated at the C-terminus. Deletion mutants of proAR suggest that the R/K-K-x-x sequence might function as an ER-retrieval signal. Disruption of this ER-retrieval-signal sequence in wild-type proAR (AR-m2) abrogated the INM targeting typically observed in response to shedding stimuli. Thus, proAR utilizes this ER retrieval signal to localize to the ER. Truncation of the cytoplasmic tail might be crucial in determination of the intracellular fate of AR-CTF compared with un-shed proAR. AR-V5-ΔC11 is localized at the nuclear envelope without shedding stimuli and decreased lamin A/C staining. AR-V5-ΔC11 is co-precipitated with anti-lamin-A/C antibody. AR-V5-ΔC10 is localized at the nuclear envelope in immunofluorescence studies; however, its effect on the lamin A/C staining and transcriptional repression is not relevant to cells expressing the wild-type proAR. Therefore we assume that removal of the 11 amino acids at the C-terminus of proAR is necessary to achieve nuclear targeting of proAR. This is the first report to describe exposure and activation of the internal ER-retrieval signal in a mammalian protein; it has been described for some protein toxins (e.g. *Pseudomonas*

exotoxin) (Sandvig and van Deurs, 2002). Accumulation of the AR-m2 mutant at the TGN suggests that proAR may translocate by way of the TGN, where truncation of the C-terminus might occur.

After translocation to the ER, proAR can diffuse laterally between the peripheral ER, ONM and INM via the nuclear pore complex, because here the cytoplasmic domain is small enough to pass through the aqueous channel. Alternatively, proAR can be translocated from the ONM to the INM via active transport, which requires protein interactions. Some integral INM proteins possess a basic-sequence motif that resembles a 'classical' nuclear localization signal (NLS) and binds to karyopherin-α (King et al., 2006). However, the cytoplasmic domain of proAR did not show any detectable NLS activity for soluble reporter proteins (data not shown).

Possible mechanism and roles for proAR-induced heterochromatin formation and transient suppression of global transcription

We observed that INM targeting of proAR triggers heterochromatin assembly and negatively regulates transcription by RNA polymerase II. Chromosomal DNA contains a high density of repetitive DNA elements, including constitutive heterochromatin. However, heterochromatin is also found at developmentally regulated loci, where the chromatin state can change in response to cellular signals and gene activity. This type of heterochromatin is known as facultative heterochromatin. The basic mechanisms that underlie proAR-induced heterochromatin formation are largely unclear. However, lamin-proAR interaction is likely to enhance the lamin-chromatin interaction because of the masking of an antigenic epitope in the chromatin-binding domain of lamin A/C. The ProAR-interacting domain in lamin A/C is shared with other lamin-A/C-binding proteins, such as the Kruppel/TFII-related zinc finger protein MOK2 (Dreuillet et al., 2002), retinoblastoma protein (Rb) (Ozaki et al., 1994) and LAP2α (Markiewicz et al., 2005), suggesting that this might have an important role in their function. Rb and LAP2 α are well known regulators of cell cycle and gene transcription in the nucleoplasm. Thus, chromatin organization might be dynamically regulated via these soluble lamin-binding proteins throughout the nucleoplasm. Furthermore, the ability of heterochromatin to spread in *cis* and to be coordinately regulated with other heterochromatin regions in *trans* may play a role in diverse heterochromatin assembly. Interestingly, the disease of premature aging, Hutchinson-Gilford Progeria Syndrome (HGPS), is caused by a 50-residue deletion mutation at the C-terminus of lamin A (LAΔ50). Nuclei in LAΔ50 mutant cells display a loss of heterochromatin, indicating that the C-terminal region of lamin A/C plays a role in chromatin organization. ProAR-dependent heterochromatin formation might be mediated via regulation of lamin function. Heterochromatinization is nearly synonymous with epigenetic gene silencing; however, there are some reports that suggest heterochromatin formation is required for activation of gene expression (Weiler and Wakimoto, 1995; Lu et al., 2000; Yasuhara and Wakimoto, 2006).

AR has been characterized as a growth factor involved in pathophysiological cell proliferation and differentiation. Thus, proAR translocation into the INM and interaction with lamin A/C, resulting in the induction of heterochromatinization and global transcriptional suppression, might participate in dynamic epigenetic reprogramming of gene expression during cell proliferation and differentiation.

Materials and Methods

Plasmids
Human *AREG* cDNA was subcloned into the *EcoRI-XhoI* sites of the pME18s vector (full-length *AREG*) or V5-tagged-pME18s vector (AR-V5). AR-V5-C was generated by insertion of a sequence encoding the V5-tag using PCR with appropriate oligonucleotide DNA primers producing the coding sequence. Mutants of truncated forms of *AREG* were generated using PCR and inserted into the *EcoRI-XhoI* sites of pME18s (AR-ΔC-V5) or pME18S-V5 (AR-ΔC1-V5~AR-ΔC4-V5). The 10- or 11-residue deletion mutant of *AREG* or AR-V5-C were generated using PCR and inserted into the *EcoRI-XhoI* sites of pME18s (AR-ΔC11, AR-V5-ΔC10, and AR-V5-ΔC11). Mutants with Ala substitutions at Lys239 and Lys240 of wild-type *AREG* (AR-m2) were generated using PCR-based site directed mutagenesis. All the cDNA constructs were verified by DNA sequencing using a CEQ 8000 DNA Analysis System (Beckman Coulter). pGEX-lamin A derivatives were gifts from Toshinori Ozaki (Ozaki et al., 1994). The plasmids pME 18S-HB-EGF-V5-C and pEGF-C1-hLAP2β were described previously (Hieda et al., 2008).

Antibodies
Affinity-purified rabbit pAbs against synthetic peptides corresponding to the cytoplasmic region of proAR (residues 233-250), i.e. AR-C pAb was obtained from Immuno Biological Laboratories (IBL). Goat pAb against the extracellular region of proAR, anti-AR-N pAb was from R&D Systems. The mouse anti-V5 mAb was from Invitrogen. Mouse anti-lamin A/C mAb (636), the mouse anti-LAMP-1 mAb (H4A3) and goat anti-lamin B pAb (M-20) were from Santa Cruz Biotechnology. Mouse anti-β-actin mAb (AC-15) was from Sigma. Sheep anti-human TGN46 pAb was from Serotec. Mouse anti-GM130 mAb was from BD Transduction Laboratories. HRP-conjugated secondary Abs were from Promega. FITC- or Cy3-conjugated secondary antibodies were from Jackson Immuno Research Laboratories. Anti-HP1β rat mAb (MAC35), anti-histone H3 dimethyl K9 mAb (1220), anti-histone H3 trimethyl K9 pAb were from Abcam. Rabbit anti-GFP pAb was from Medical & Biological Laboratories (MBL).

Preparation of monoclonal antibodies
Monoclonal antibodies were generated using the rat lymph node method (Sado et al., 1995). Briefly, WKY/Ncrj rats (Charles River Japan) were immunized with an emulsion containing a KLH-conjugated synthetic peptide, which corresponds to that of the cytoplasmic region of AR, and Freund's complete adjuvant. Cells from the lymph nodes were fused with mouse myeloma Sp2/0 cells. The hybridomas were screened using ELISA and three clones (No.2, No.5 and No.9) were established. The isotype subclass of mAb2, mAb5 and mAb9 were determined to be IgM, IgG2b and IgG1, respectively, using a rat monoclonal antibody ID/SP Kit (Zymed Laboratories).

Cell culture, transfection and TPA treatment
HeLa cells were grown in DMEM (Nikken Biomedical Laboratory) supplemented with 10% fetal bovine serum (HyClone). Transfections were performed using Lipofectamine™ 2000 (Invitrogen). For induction of the shedding process, cells were incubated with 100 nM TPA for 30 minutes, unless otherwise indicated in the figure legends.

Digitonin permeabilization
For digitonin permeabilization, the cells were incubated with transport buffer (20 mM HEPES pH 7.3, 110 mM potassium acetate, 5 mM sodium acetate, 2 mM magnesium acetate, 1 mM EDTA and 2 mM DTT) containing 33 μg/ml digitonin on ice for 5 minutes. After permeabilization, cells were washed and fixed with 4% paraformaldehyde in transport buffer.

Preparation of cell lysate
Cells were lysed in ice-cold lysis buffer, PBS (−) containing 50 mM Tris-HCl pH 7.5, 150 mM NaCl, 1% Triton X-100, and protease inhibitor cocktail (Roche). Cell lysates were incubated for 30 minutes at 4°C and centrifuged at 9100 *g* for 10 minutes. The resulting supernatants were used as total cell lysates.

Immunoprecipitation
Total cell lysates were incubated with anti-lamin A/C mAb for 2 hours at 4°C. Protein-G-Sepharose beads (Amersham Biosciences) were then added to the mixture. After incubation for 1 hour, the suspension was centrifuged, and the collected protein-G-Sepharose beads were washed three times with lysis buffer. The bound proteins were analyzed by western blotting.

GST pull-down assays
GST and GST-lamin mutants were produced in and purified from *E. coli*, as described previously (Ozaki et al., 1994). Total cell lysates were mixed with 2 μg recombinant GST or GST-lamin mutants and glutathione-Sepharose beads for 2 hours at 4°C. The bound proteins were analyzed by SDS-PAGE, followed by western blotting.

Immunofluorescence microscopy
Cells were fixed with 4% paraformaldehyde for 20 minutes and permeabilized with 0.2% Triton X-100 for 10 minutes at room temperature. Cells were blocked with 2% BSA and incubated with primary antibodies overnight at 4°C. Cells were viewed with an epifluorescence microscope (IX70, Olympus).

siRNA knockdown
A specific RNA dimer that targets the coding sequence of human A-type lamin at nucleotides 608-626 was obtained from Dharmacon. Specific RNA dimers corresponding to B-type lamins, lamin B1 and lamin B2 (Tsai et al., 2006) were obtained from B-Bridge International. RNA dimers were transfected into HeLa cells using Lipofectamine2000 (Invitrogen).

Br-U incorporation and its quantification
Cells were grown in 5 mM Br-U for 30 minutes and fixed with 4% paraformaldehyde. Br-RNA was immunolabeled using a rat anti-BrdU mAb (Abcam). The fluorescent intensity in the nucleus was measured in 200 cells with Image-pro plus (MediaCybernetics). The analysis was performed in triplicate and results were considered significant at a level of *P*<0.05.

Nuclear extraction
HeLa cells transiently expressing proAR were extracted using a protocol described previously (Markiewicz et al., 2005) with some modifications. Cells were rinsed twice with TM buffer (20 mM Tris-HCl pH 7.5, 3 mM MgCl$_2$) and then incubated for 10 minutes on ice in TM buffer containing 0.4% Triton X-100, 0.5 mM CuCl$_2$ and proteinase inhibitors. After washing with TM buffer, cells were incubated with DNase I (20 U/ml) for 20 minutes at 37°C, or/and incubated with 2 M NaCl for 5 minutes on ice.

Immunogold electron microscopy
The cells were fixed with 2% paraformaldehyde/0.25% glutaraldehyde, dehydrated and embedded in LR White resin. Ultrathin sections were blocked with 1% BSA and incubated in anti-V5 mAb. The bound antibody was detected using gold-conjugated anti-mouse IgG (15 nm; BBInternational, UK). After incubation, the grids were counterstained with 2% uranyl acetate and lead citrate and examined with a JEOL JEM1230 transmission electron microscope.

References
Adam, S. A., Marr, R. S. and Gerace, L. (1990). Nuclear protein import in permeabilized mammalian cells requires soluble cytoplasmic factors. *J. Cell Biol.* **111**, 807-816.

Anklesaria, P., Teixidó, J., Laiho, M., Pierce, J. H., Greenberger, J. S. and Massagué, J. (1990). Cell-cell adhesion mediated by binding of membrane-anchored transforming growth factor alpha to epidermal growth factor receptors promotes cell proliferation. *Proc. Natl. Acad. Sci. USA* **87**, 3289-3293.

Blobel, C. P. (2005). ADAMs: key components in EGFR signaling and development. *Nat. Rev. Mol. Cell. Biol.* **6**, 32-43.

Dreuillet, C., Tillit, J., Kress, M. and Ernoult-Lange, M. (2002). *In vivo* and *in vitro* interaction between human transcription factor MOK2 and nuclear lamin A/C. *Nucleic Acids Res.* **30**, 4634-4642.

Dyer, J. A., Kill, I. R., Pugh, G., Quinlan, R. A., Lane, E. B. and Hutchison, C. J. (1997). Cell cycle changes in A-type lamin associations detected in human dermal fibroblasts using monoclonal antibodies. *Chromosome Res.* **6**, 383-394.

Goldman, R. D., Gruenbaum, Y., Moir, R. D., Shumaker, D. K. and Spann, T. P. (2002). Nuclear lamins: building blocks of nuclear architecture. *Genes. Dev.* **16**, 533-547.

Gruenbaum, Y., Margalit, A., Goldman, R. D., Shumaker, D. K. and Wilson, K. L. (2005). The nuclear lamina comes of age. *Nat. Rev. Mol. Cell. Biol.* **6**, 21-31.

Hieda, M., Isokane, M., Koizumi, M., Higashi, C., Tachibana, T., Shudou, M., Taguchi, T., Hieda, Y. and Higashiyama, S. (2008). Membrane-anchored growth factor, HB-EGF, on the cell surface targeted to the inner nuclear membrane. *J. Cell Biol.* **180**, 763-769.

Higashiyama, S., Iwamoto, R., Goishi, K., Raab, G., Taniguchi, N., Klagsbrun, M. and Mekada, E. (1995). The membrane protein CD9/DRAP 27 potentiates the juxtacrine

growth factor activity of the membrane-anchored heparin-binding EGF-like growth factor. *J. Cell Biol.* **128**, 929-938.

Higashiyama, S., Iwabuki, H., Morimoto, C., Hieda, M., Inoue, H. and Matsushita, N. (2008). Membrane-anchored growth factors, the EGF family: beyond receptor ligands. *Cancer Sci.* **99**, 214-220.

Hinkle, C. L., Sunnarborg, S. W., Loiselle, D., Parker, C. E., Stevenson, M., Russell, W. E. and Lee, D. C. (2004). Selective roles for tumor necrosis factor alpha-converting enzyme/ADAM17 in the shedding of the epidermal growth factor receptor ligand family: the juxtamembrane stalk determines cleavage efficiency. *J. Biol. Chem.* **279**, 24179-24188.

Holmer, L. and Worman, H. J. (2001). Inner nuclear membrane proteins: functions and targeting. *Cell Mol. Life Sci.* **58**, 1741-1747.

Hozák, P., Sasseville, A. M., Raymond, Y. and Cook, P. R. (1995). Lamin proteins form an internal nucleoskeleton as well as a peripheral lamina in human cells. *J. Cell Sci.* **108**, 635-644.

Iborra, F. J., Jackson, D. A. and Cook, P. R. (1998). The path of transcripts from extranucleolar synthetic sites to nuclear pores: transcripts in transit are concentrated in discrete structures containing SR proteins. *J. Cell Sci.* **111**, 2269-2282.

Jackson, M. R., Nilsson, T. and Peterson, P. A. (1990). Identification of a consensus motif for retention of transmembrane proteins in the endoplasmic reticulum. *EMBO J.* **9**, 3153-3162.

King, M. C., Lusk, C. P. and Blobel, G. (2006). Karyopherin-mediated import of integral inner nuclear membrane proteins. *Nature* **442**, 1003-1007.

Kinugasa, Y., Hieda, M., Hori, M. and Higashiyama, S. (2007). The carboxyl-terminal fragment of pro-HB-EGF reverses Bcl6-mediated gene repression. *J. Biol. Chem.* **282**, 14797-14806.

Koberna, K., Stanek, D., Malínský, J., Eltsov, M., Pliss, A., Ctrnáctá, V., Cermanová, S. and Raska, I. (1999). Nuclear organization studied with the help of a hypotonic shift: its use permits hydrophilic molecules to enter into living cells *Chromosoma* **108**, 325-333.

Kumaran, R. I., Muralikrishna, B. and Parnaik, V. K. (2002). Lamin A/C speckles mediate spatial organization of splicing factor compartments and RNA polymerase II transcription. *J. Cell Biol.* **159**, 783-793.

Lu, B. Y., Emtage, P. C., Duyf, B. J., Hilliker, A. J. and Eissenberg, J. C. (2000). Heterochromatin protein 1 is required for the normal expression of two heterochromatin genes in *Drosophila. Genetics* **155**, 699-708.

Markiewicz, E., Ledran, M. and Hutchison C. J. (2005). Remodelling of the nuclear lamina and nucleoskeleton is required for skeletal muscle differentiation in vitro. *J. Cell Sci.* **118**, 409-420.

Mounkes, L., Kozlov, S., Burke, B. and Stewart, C. L. (2003). The laminopathies: nuclear structure meets disease. *Curr. Opin. Genet. Dev.* **13**, 223-230.

Nanba, D., Mammoto, A., Hashimoto, K. and Higashiyama, S. (2003). Proteolytic release of the carboxy-terminal fragment of proHB-EGF causes nuclear export of PLZF. *J. Cell Biol.* **163**, 489-502.

Nilsson, T., Jackson, M. and Peterson, P. A. (1989). Short cytoplasmic sequences serve as retention signals for transmembrane proteins in the endoplasmic reticulum. *Cell* **58**, 707-718.

Ozaki, T., Saijo, M., Murakami, K., Enomoto, H., Taya, Y. and Sakiyama, S. (1994). Complex formation between lamin A and the retinoblastoma gene product: identification of the domain on lamin A required for its interaction. *Oncogene* **9**, 2649-2653.

Plowman, G. D., Green, J. M., McDonald, V. L., Neubauer, M. G., Disteche, C. M., Todaro, G. J. and Shoyab, M. (1990). The amphiregulin gene encodes a novel epidermal growth factor-related protein with tumor-inhibitory activity. *Mol. Cell. Biol.* **10**, 1969-1981.

Rozengurt, E. (2007). Mitogenic signaling pathways induced by G protein-coupled receptors. *J. Cell Physiol.* **213**, 589-602.

Sado, Y., Kagawa, M., Kishiro, Y., Sugihara, K., Naito, I., Seyer, J. M., Sugimoto, M., Oohashi, T. and Ninomiya, Y. (1995). Establishment by the rat lymph node method of epitope-defined monoclonal antibodies recognizing the six different alpha chains of human type IV collagen. *Histochem. Cell Biol.* **104**, 267-275.

Sahin, U., Weskamp, G., Kelly, K., Zhou, H. M., Higashiyama, S., Peschon, J., Hartmann, D., Saftig, P. and Blobel, C. P. (2004). Distinct roles for ADAM10 and ADAM17 in ectodomain shedding of six EGFR ligands. *J. Cell Biol.* **164**, 69-79.

Sandvig, K. and van Deurs, B. (2002). Transport of protein toxins into cells: pathways used by ricin, cholera toxin and Shiga toxin. *FEBS Lett.* **529**, 49-53.

Schirmer, E. C., Florens, L., Guan, T., Yates, J. R. and Gerace, L. (2003). Nuclear membrane proteins with potential disease links found by subtractive proteomics. *Science* **301**, 1380-1382.

Singh, A. B. and Harris, R. C. (2005). Autocrine, paracrine and juxtacrine signaling by EGFR ligands. *Cell Signal* **17**, 1183-1193.

Spann, T. P., Moir, R. D., Goldman, A. E., Stick, R. and Goldman, R. D. (1997). Disruption of nuclear lamin organization alters the distribution of replication factors and inhibits DNA synthesis. *J. Cell Biol.* **136**, 1201-1212.

Spann, T. P., Goldman, A. E., Wang, C., Huang, S. and Goldman, R. D. (2002). Alteration of nuclear lamin organization inhibits RNA polymerase II-dependent transcription. *J. Cell Biol.* **156**, 603-608.

Tokumaru, S., Higashiyama, S., Endo, T., Nakagawa, T., Miyagawa, J. I., Yamamori, K., Hanakawa, Y., Ohmoto, H., Yoshino, K., Shirakata, Y. et al. (2000). Ectodomain shedding of epidermal growth factor receptor ligands is required for keratinocyte migration in cutaneous wound healing. *J. Cell Biol.* **151**, 209-220.

Tsai, M. Y., Wang, S., Heidinger, J. M., Shumaker, D. K., Adam, S. A., Goldman, R. D. and Zheng, Y. (2006). A mitotic Lamin B matrix induced by RanGTP required for spindle assembly. *Science* **311**, 1887-1893.

Vlcek, S., Dechat, T. and Foisner, R. (2001). Nuclear envelope and nuclear matrix: interactions and dynamics. *Cell Mol. Life Sci.* **58**, 1758-1765.

Weiler, K. S. and Wakimoto, B. T. (1995). Heterochromatin and gene expression in *Drosophila. Annu. Rev. Genet.* **29**, 577-605.

Yasuhara, J. C. and Wakimoto, B. T. (2006). Oxymoron no more: the expanding world of heterochromatic genes. *Trends Genet.* **22**, 330-338.

Zastrow, M. S., Vlcek, S. and Wilson, K. L. (2004). Proteins that bind A-type lamins: integrating isolated clues. *J. Cell Sci.* **117**, 979-987.